

# Saving Planetary Systems: Dead Zones & Planetary Migration

Soko Matsumura<sup>1</sup>, Ralph E. Pudritz<sup>2</sup>

*Department of Physics & Astronomy, McMaster University, Hamilton, ON L8S 4M1,  
Canada*

soko@physics.mcmaster.ca, pudritz@physics.mcmaster.ca

and

Edward W. Thommes

*Canadian Institute for Theoretical Astrophysics, University of Toronto, 60 St. George  
Street, Toronto, ON M5S 3H8, Canada*

thommes@cita.utoronto.ca

## ABSTRACT

The tidal interaction between a disk and a planet leads to the planet's migration. It is widely believed that this mechanism explains the variety of orbital radii of extrasolar planets. A long-standing question regarding this mechanism is how to stop the migration before planets plunge into their central stars.

In this paper, we propose a new, simple mechanism to significantly slow down planet migration, and test the possibility by using a hybrid numerical integrator to simulate the disk-planet interaction. The key component of the scenario is the role of low viscosity regions in protostellar disks known as dead zones. A region of low viscosity affects planetary migration in two ways. First of all, it allows a smaller-mass planet to open a gap, and hence switch the faster type I migration (pre-gap-opening migration) to the slower type II migration (post-gap-opening migration). Secondly, a low viscosity slows down type II migration itself, because type II migration is directly proportional to the viscosity.

We present numerical simulations of planetary migration in disks by using a hybrid symplectic integrator-gas dynamics code. Assuming that the disk viscosity

---

<sup>1</sup>Current location: Department of Physics & Astronomy, Northwestern University, 2145 Sheridan Road, Evanston, IL 60208-0834, USA, e-mail: soko@northwestern.edu

<sup>2</sup>Origins Institute, ABB 241, McMaster University, 1280 Main Street West, Hamilton, ON, L8S 4M1, Canada

parameter inside the dead zone is  $\alpha = 10^{-4} - 10^{-5}$ , we find that, when a low-mass planet (e.g. 1 - 10 Earth masses) migrates from outside the dead zone, its migration is stopped due to the mass accumulation inside the dead zone. When a low-mass planet migrates from inside the dead zone, it opens a gap and slows down its migration. A massive planet like Jupiter, on the other hand, opens a gap and slows down inside the dead zone, independent of its initial orbital radius. The final orbital radius of a Jupiter mass planet depends on the dead zone’s viscosity. For the range of  $\alpha$ ’s noted above, this can vary anywhere from 7 AU, to an orbital radius of 0.1 AU that is characteristic of the hot Jupiters.

## 1. Introduction

Since the first discovery of an extrasolar planet around a solar-type star in 1995 (Mayor & Queloz 1995), surveys for extrasolar planets have sampled several thousand solar-type stars. Out of these, at least 5 – 25% harbor Jupiter mass planets within  $\sim 5$  AU of their central stars (e.g. Lineweaver & Grether 2003; Butler et al. 2006). Most extrasolar planets are of Jupiter mass  $M_J$ , or even larger (up to  $\sim 10M_J$ ), and tend to orbit very close to the central star — sometimes even closer than Mercury is to the Sun (e.g. Udry et al. 2003). These close-in planets, which have orbital radii less than about 0.1 AU, are called “hot Jupiters” (e.g. Mayor & Queloz 1995; Marcy & Butler 1996; Santos et al. 2005). Arguably the best explanation that we have for these planets is that they were formed further out in the disks, and then migrated to the current locations (e.g. Goldreich & Tremaine 1980; Lin & Papaloizou 1993; Ward 1997; Masset & Papaloizou 2003; Artymowicz 2004). This raises several interesting questions about the evolution of planetary systems. As an example, does the current estimate of the percentage of stars harboring planets represent the overall probability of a planetary system to survive, or does it rather suggest that only in 5 – 25% of cases planetary systems undergo enough migration to place Jupiter-like planets within 5 AU? In this latter view, there would be more planets beyond 5 AU, waiting to be detected in future programs.

The problem with migration as it is currently understood, is that planet-disk interaction is too efficient. Planets rapidly migrate within a gaseous disk and plunge into their central stars in less than a few million years for disk models with standard values of the disk viscosity. This raises the question of whether or not planetary systems typically survive at all. In this work, we will demonstrate that dead zones (low viscosity regions in disks) play a crucial role in saving planetary systems by significantly slowing planetary migration.

Planets migrate as they tidally interact and exchange angular momentum with their disk at Lindblad or corotation resonances. The different kinds of planet migration that

arise are generally divided into three types (type I, II, and III). Type I migration occurs for planets that are not massive enough to open a gap in protostellar disks (e.g. Earth mass and 10 Earth mass planets). Such planets most strongly interact with the disk at Lindblad resonances, and hence the effect of corotation torque is negligible (e.g. Goldreich & Tremaine 1980). Usually, planets feel a stronger outer torque than an inner torque, and thus the total torque is negative and the overall migration is inward, relative to the disk. The migration speed is proportional to the planetary mass  $M_p$ , disk surface mass density  $\Sigma$ , and inversely proportional to the square of the disk aspect ratio  $h/r$ , where  $h$  is the pressure scale height and  $r$  is the disk radius (e.g. Goldreich & Tremaine 1980; Lin & Papaloizou 1993; Ward 1997).

Type II migration occurs for planets that are massive enough to open a clear gap in the disks (roughly Jupiter mass and up). Such planets are locked in the gap, and coupled to the disk through the Lindblad resonances which are distant enough from the planets to fall beyond the gap edge. They migrate as the gaseous disk accretes toward the central star due to the disk’s viscosity. As long as the disk mass is large compared to the planet mass, the migration speed is proportional to the disk’s viscosity parameter  $\alpha$  and the square of the disk’s aspect ratio. Type II migration is generally one to two orders of magnitude slower than type I migration (Ward 1997).

Finally, type III migration pertains to planets with an intermediate mass (e.g. Saturn mass planets), which are just heavy enough to start opening a gap. These planets feel the effect of a sharp transition of the surface mass density at the edges of gaps. Since the corotation torque is proportional to the surface mass density gradient (e.g. Goldreich & Tremaine 1979; Tanaka et al. 2002), its effect dominates the exchange of angular momentum between a planet and a disk. The angular momentum is transferred as the disk material which is trapped in horseshoe orbits passes by the planet. This may lead to a rapid inward or outward migration depending on the initial migration direction of the planet (e.g. Goldreich & Tremaine 1980; Ward 1992; Masset & Papaloizou 2003; Artymowicz 2004). The migration speed is comparable to the type I migration (Masset & Papaloizou 2003).

For standard disk models, all types of migration are primarily inward, and their timescale is at least one to two orders of magnitude shorter than the disk’s lifetime ( $10^6 - 10^7$  years). Therefore, in order to avoid being swallowed by their central stars, the planets’ migration has to be significantly slowed down or stopped somehow. Otherwise, giant planets would only have a chance to form once the gas disk is already significantly depleted (Thommes & Murray 2006).

A number of scenarios have been proposed to solve this problem. Some scenarios stop planet migration very close to the central stars either by an inner magnetospheric cavity

in the disk (e.g. Shu et al. 1994; Lin et al. 1996), or by the tidal interaction with the star (e.g. Lin et al. 1996). Also, an overflow of the Roche lobe between the central star and a planet could reverse planet migration (Trilling et al. 1998), because a planet loses mass to the central star and therefore moves outward to conserve the angular momentum of the system. However, these mechanisms cannot explain the planets orbiting farther than the immediate vicinity of the star.

Another scenario predicts that the planets stop migration when they move from a non-magnetized region of a disk into a magnetized region (Terquem 2003). This is because the outer torque due to the magnetic resonances disappears in such a case, and because the contribution from the magnetic resonances dominates that from the Lindblad resonances. This mechanism, however, cannot stop type II planet migration.

The torque fluctuations due to the magnetorotational instability (MRI) turbulence which were recently discovered in numerical simulations (e.g. Laughlin et al. 2004; Nelson & Papaloizou 2004; Nelson 2005) may be able to prolong the lifetime of some planets (Johnson et al. 2006). This mechanism, however, won't be able to explain the survival of planets heavier than about 10 Earth masses.

We show in this paper that dead zones can stop or slow down planetary migration very efficiently. The underlying assumption here is that the major source of disk's viscosity is the magnetorotational instability (MRI) turbulence (e.g. Balbus & Hawley 1991). A dead zone is a dense region in a disk which is poorly ionized, and hence MRI inactive and nearly inviscid (e.g. Gammie 1996). Although typical disks are expected to have dead zones (e.g. Gammie 1996; Glassgold et al. 1997; Sano et al. 2000; Fromang et al. 2002; Semenov et al. 2004; Matsumura & Pudritz 2003, 2005, 2006, hereafter MP03, MP05, and MP06 respectively), their effect on the evolution of protostellar systems has received little attention. Since the disk's viscosity affects the rate of planetary migration, and since planet formation occurs concurrently with migration, it is important to take account of such variations in disk's viscosity.

In this paper, we study planet migration in disks with dead zones by means of state of the art numerical simulations as well as analytical calculations. We first introduce our disk models and numerical methods, and show the disk evolution with a dead zone in §2. Then we consider the case of planetary migration beginning from beyond the dead zone, and compare it with the case of disks with no dead zone (§3). We then present the planet migration from inside the dead zone, focusing on a width of the gap opened by a planet in §4. The migration in disks with various viscosity parameters is briefly discussed in §5. Finally, the discussion and conclusion are presented in §6.

## 2. Disk Models & Numerical Simulations

### 2.1. Numerical methods

We perform numerical simulations of planet migration in protostellar disks using a hybrid numerical code, which combines an N-body integrator with a simple disk model (Thommes 2005). The N-body part is based on the symplectic integrator SyMBA (Duncan et al. 1998), which applies the method of Wisdom & Holman (1991) with an adaptive timestep to resolve close encounters between massive bodies. The disk part of the code evolves viscously as well as through angular momentum exchange with the embedded planets.

In this code, the disk is treated as one-dimensional in the radial direction, so the disk properties are averaged vertically and azimuthally. However, three-dimensional effects are implicitly included in the code — the vertical direction effect comes in through the pressure scale height (or equivalently, the sound speed) and the azimuthal direction through the torque density, which represents the effect of azimuthally asymmetric structure, i.e. the spiral density waves launched at Lindblad resonances (see Appendix B).

By combining the continuity and angular momentum equations, the evolution of the surface mass density of a disk is calculated as follows (e.g. Pringle 1981):

$$\frac{\partial \Sigma}{\partial t} = \frac{1}{2\pi r} \frac{\partial}{\partial r} \left[ \left[ \frac{\partial}{\partial r} (\Omega r^2) \right]^{-1} \frac{\partial}{\partial r} (T_{\text{viscous}} - T_{\text{tidal}}) \right], \quad (1)$$

where  $T_{\text{viscous}} = 3\pi r^2 \nu \Sigma_{\text{gas}} \Omega$  is the viscous torque ( $\nu = \alpha c_s h$  is the viscosity,  $\Sigma_{\text{gas}}$  is the gas surface mass density, and  $\Omega$  is the orbital frequency), and  $T_{\text{tidal}}$  is the tidal torque (see Appendix B for an expression). Since planetary migration is mainly affected by the principal Lindblad resonances (e.g. Goldreich & Tremaine 1980; Ward 1997), we neglect higher order resonances as well as corotation resonances. We assume a nearly Keplerian disk  $\kappa \sim \Omega$ , and therefore calculate the tidal torque between the 2:1 and 1:2 resonances. Planetary eccentricities are assumed to be nearly zero throughout this paper.

Each time step of the above equation is solved in three steps. First, the disk is evolved due to only the viscous diffusion (e.g. under the influence of the first term in Eq. 2 alone) for half a time step. Then it is evolved due to the planet-disk interaction (e.g. under the influence of the second term) for a full time step. Finally, the disk is evolved for another half a time step under the influence of the viscous diffusion. The planet’s orbit is calculated three dimensionally in a similar manner.

## 2.2. Initial Conditions

We set up the initial disks based on our previous work (MP06). We consider both disks with and without dead zones. For the former case, we use the dead zone radii which were obtained in our previous work, and assume the lower viscosity parameter inside the dead zones.

Since the detailed explanation of our disk models and the way we determined the size of the dead zones are documented elsewhere (MP03, MP05, and MP06), we simply summarize our previous results here.

MP06 showed that a typical dead zone extends from 0.04 to 13 AU in protostellar disks. Since the size of the dead zones depend on both the thermal and ionization structure of disks, we used the disk models which reproduce the observed spectral energy distributions (SEDs) very well (Chiang et al. 2001; Robberto et al. 2002), and calculated the electron density within them (see MP03, MP05 as well). We took account of the ionization by X-rays from the central stars, cosmic rays, radioactive elements, and thermal collisions of alkali ions, as well as the recombination by molecular ions, metals, and grains. The innermost disk (less than about 0.04 AU) is magnetically active since the collisional ionization is efficient, and since grains, which are an efficient recombination source, are evaporated due to the high temperature there. The outer part of the disks (larger than about 13 AU) are magnetically active since the disks are less dense, and therefore well-ionized. Similar work done by Semenov et al. (2004) gives roughly the same results. For simplicity, we assume that the disk within 13 AU is dead in this paper (see also §6).

Throughout this paper, we use a fiducial value for the viscosity parameter  $\alpha = 10^{-5}$  for inside the dead zones, and  $\alpha = 10^{-2}$  for outside it (active zones). These values agree well with the three-dimensional numerical MHD simulations of the layered accretion disks done by Fleming & Stone (2003). We note however that real disks may have a significant range for the viscosity parameter centered on these fiducial values (see §5).

The initial disks have a gas surface mass density structure of  $\Sigma_{gas} = \Sigma_{0,gas}(r/AU)^{-3/2}$  where  $\Sigma_{0,gas} = 10^3 \text{ g cm}^{-2}$ , and the temperature structure of disk models by Robberto et al. (2002). We assumed the solid surface mass density of  $\Sigma_{solid} = \Sigma_{0,solid}(r/AU)^{-2}$  where  $\Sigma_{0,solid} = 270 \text{ g cm}^{-2}$ , following Pollack et al. (1996) and Alibert et al. (2005). Although the solid materials or planetesimals don't directly affect the results of the current paper, they will become important during the formation of planets in disks with dead zones. We will discuss this in a subsequent paper.

We perform simulations on only low-mass planets (1 and 10 Earth mass planets) and massive planets (1 Jupiter mass planet). We don't take account of type III migration, which

is shown to be effective for intermediate mass planets like Saturn (e.g. Goldreich & Tremaine 1980; Ward 1992; Masset & Papaloizou 2003; Artymowicz 2004). This is because there has been no reliable way as yet to evaluate the corotation torque in an azimuthally averaged way.

### 2.3. The dead zone’s effects on disk surface mass density

We first show how a dead zone with a fixed radius would change the disk’s surface mass density profile. Here, we consider the disk with no planets. We assume that the initial surface mass density has a smooth power law distribution ( $\Sigma \propto r^{-3/2}$ , see the last subsection), and that the viscosity parameter is  $\alpha = 10^{-5}$  inside the dead zone radius  $r_{DZ} = 13$  AU, and  $\alpha = 10^{-2}$  outside it.

Our main assumptions are (1) the dead zone has a fixed outer radius (typically,  $r_{DZ} = 13$  AU), (2) the temperature profile does not change throughout the simulation, and (3) there is no surface layer accretion. Naturally, each of these factors affects disk evolution significantly. We will discuss this issue in a subsequent paper. Here, we merely consider a simplified model, which captures a trend of the evolution of such a disk, and discuss the effects of a dead zone on planet migration.

Fig. 1 shows the evolution of the disk’s surface mass density. Since the mass accretion speed is proportional to the viscosity parameter  $\alpha$ , the disk outside a dead zone accretes three orders of magnitude faster than the dead zone. Therefore, the disk quickly develops a steep surface mass density gradient at this radius (within  $t \sim 10^4$  years). The mass accreting from outside the dead zone accumulates at the edge of the dead zone, and slowly spreads over the dead zone. This mass accumulation makes a jump in the surface mass density profile, which eventually reaches a three to four orders of magnitude difference between dead and active zones <sup>1</sup>

When the surface mass density increases as seen in the simulation, the disk becomes optically thick, and therefore the ionization rates decrease. This ensures that a dead zone is even more “dead”, because the MRI turbulence requires a disk to be well-ionized. We can estimate dead zone’s effects on planet migration as follows. Assuming a vertical hydrostatic equilibrium for an ideal gas, we can write the disk aspect ratio as  $h/r = \sqrt{(T/T_c)(r/R_*)}$

---

<sup>1</sup>It should be pointed out that such a steep density jump makes a disk locally Rayleigh unstable ( $\kappa^2 < 0$ , see Appendix B for an expression). This is likely to reduce the gradient of surface mass density somewhat. We will leave this as a future work.

where  $T_c = k_B R_*/(GM_* \mu m_H)$  ( $k_B$  is Boltzmann constant,  $G$  is the gravitational constant,  $\mu$  is the mean molecular weight,  $m_H$  is the hydrogen mass, and  $R_*$  and  $M_*$  are stellar radius and mass respectively). With this, the type I and type II migration speeds can be written as (e.g. Ward 1997):

$$v_{\text{typeI}} \propto -2 \frac{M_p}{M_*} (r_p \Omega_p) \frac{\pi \Sigma_p r_p^2}{M_*} \left( \frac{T_p r_p}{T_c R_*} \right)^{-1} \quad (2)$$

$$v_{\text{typeII}} = -\frac{3}{2} \alpha (r_p \Omega_p) \left( \frac{T_p r_p}{T_c R_*} \right), \quad (3)$$

where the subscript  $p$  indicates that the values are evaluated at a planet's orbital radius  $r_p$ . In typical protostellar disks, two order of magnitude increase in surface mass density leads to a factor of a few increase in temperature (e.g. Lecar et al. 2006), and hence the temperature evolution is negligible compared to the surface mass density evolution. Since the surface mass density increases inside the dead zone, the type I migration speed there is expected to be *faster* than that outside the dead zone. On the other hand, the type II migration speed is expected to be *slower*, because the disk's viscosity parameter  $\alpha$  is smaller. Therefore, we expect that at least type II migration is slowed inside a dead zone.

Another important effect of a dead zone on planet migration is that the gap-opening mass becomes very small inside a dead zone. Fig. 2 shows the gap-opening mass in our initial disk model with a dead zone. The upper dashed line shows the gap-opening mass expected for a viscous disk with  $\alpha = 10^{-2}$ , while the lower dashed line shows that for an inviscid disk. A solid line is the expected gap-opening mass throughout the disk. Outside the dead zone, planets open gaps when the tidal torque exceeds the viscous torque (e.g. Lin & Papaloizou 1993; Bryden et al. 1999):

$$\frac{M_p}{M_*} \gtrsim \sqrt{40\alpha} \left( \frac{h_p}{r_p} \right)^5, \quad (4)$$

which represents the upper dashed line. Outside the dead zone, this corresponds to Jupiter or larger mass planets. On the other hand, these results show that even a terrestrial mass planet can open a gap inside the dead zone, since the viscosity there is very small. The gap-opening mass in a gravitationally stable, low viscosity disk ( $\alpha \sim 10^{-5}$ ) is well approximated by that in an inviscid disk with a reasonable disk aspect ratio  $h/r \gtrsim 0.02$  (Rafikov 2002):

$$\frac{M_p}{M_*} \gtrsim \frac{2}{3} \left( \frac{h_p}{r_p} \right)^3 \min \left[ 5.2 Q^{-5/7}, 3.8 \left( Q \frac{r_p}{h_p} \right)^{-5/13} \right], \quad (5)$$

which represents the lower dashed line. Here, we see the gap-opening mass reaches an Earth mass at  $\sim 0.7$  AU. Therefore, we expect that a planet with  $M_E$  or  $10M_E$  opens a gap inside a dead zone, and hence migrates at a slower type II rate afterwards.



These terrestrial, gap-opening planets may execute type III migration instead of type II migration inside the dead zone. In such a case, these planets may migrate rapidly, at about one-third of the type I migration rate (Masset & Papaloizou 2003). If it were the case, the planets would be trapped at the inner edge of the dead zone due to the positive corotation torque (Masset et al. 2006). In our dead zone with  $\alpha \sim 10^{-5}$ , type III migration is unlikely because the corotation torque tends to saturate in such a low viscosity disk. We show this analytically in Appendix A.

When planets are migrating from outside the dead zone, the situation is more complicated. The density jump affects both Lindblad and corotation torques. For the former case, the inner torque becomes larger, because the torque is proportional to the surface mass density. If the density increase is large enough, the inner torque exceeds the outer torque in magnitude, and the differential torque becomes positive — i.e. planet migration is directed *outward*. We present a detailed analysis of this result in Appendix B. On the other hand, for the corotation torque, such a sharp surface mass density gradient would increase the amount of material that gets caught in the inner horseshoe orbit, and hence lead to the rapid *inward* migration. Therefore, we need to evaluate both Lindblad and corotation torques to determine the exact direction of migration. However, we will show in Appendix B that the positive Lindblad torque starts acting far away from the density jump. Since the corotation torque has a significant effect only at the density jump, it is likely that the overall migration is directed outward due to the positive net Lindblad torque. Therefore, we only take account of the effect of the Lindblad torque in our calculation.

In the following sections, we follow planetary migration from an initial orbit in which a planet is outside the dead zone (§3) as well as inside the dead zone (§4).

### 3. Planet migration from outside the dead zones

Here, we will focus on the migration of planets whose initial orbits are outside the dead zone. Since a dead zone evolves much slower than the disk annuli outside it, there should be a mass accumulation inside the dead zone as seen in the last section. The resulting jump in surface density at the zone’s outer edge can stop the migration of the planet.

### 3.1. Hybrid numerical simulations of planetary migration from outside the dead zone

We compute planetary migration towards the dead zone for different mass planets, namely those with 1 Earth mass, 10 Earth masses, and 1 Jupiter mass. We choose their initial orbital radius to be 20 AU, so that we can ensure that a density jump fully develops before planets approach the effective range of a surface mass density jump, and that even a Jupiter mass planet starts as a type I migrator. Since massive planets probably form much closer-in, the migration rates we compute are upper limits.

The former point is justified by Appendix B. The results in Fig. 13 and 14 suggest that planets start feeling the effect of the mass accumulation from radii  $13 \text{ AU} < r_p < 18.5 \text{ AU}$  ( $0.7 < r_{\text{edge}}/r_p < 1$  with  $r_{\text{edge}} = 13 \text{ AU}$ ), depending on the steepness and magnitude of a density jump as well as the disk thickness.

The latter point can be easily seen from Fig. 2. For a disk with  $\alpha = 10^{-2}$ , the gap-opening mass at 20 AU is larger than  $1M_J$  (see the upper line). Therefore, all planets start as type I migrators.

We first show the case for an Earth mass planet in Fig. 3. The left panel of Fig. 3 shows the migration of a 1 Earth mass planet in a disk *without* a dead zone (i.e. the viscosity has the parameter  $\alpha = 10^{-2}$  everywhere). The y-axis shows the radius of the disk, and the x-axis shows its time evolution. Also shown are the contours of the disk’s surface mass density. By examining these contours, we can tell that the disk is accreting toward the central star ( $y=0$ ) as time goes on (toward right on the x-axis). The thick black line is semi-major axis of the orbit of the planet, which starts migrating from 20 AU. It is apparent that the planet plunges into the star within about  $5 \times 10^6$  years (note that the migration rate decreases with semimajor axis). This migration time roughly agrees with the one expected from the theory ( $\sim 2 \times 10^6$  years, see e.g. Ward 1997); the softening parameter, which mimics the reduction of a torque with vertical height ( $B = 0.2$ , see Appendix B as well), contributes to making it longer.

The right panel of Fig. 3 is the analogous figure for a disk *with* a dead zone (i.e. the viscosity parameter  $\alpha = 10^{-5}$  inside and  $10^{-2}$  outside the dead zone). In this run, an Earth mass planet starts migrating from 20 AU, just outside the outer dead zone radius 13 AU. As expected from the previous section, the inward migration is halted before the planet reaches the outer edge of the dead zone, and then the planet starts migrating outward. When the planet moves away from the surface mass density jump, the inner and outer tidal torques balance, and the planet migration stops at around  $\sim 19.8 \text{ AU}$ . The simulations were checked until they converged, by using smaller and smaller radial steps.

These results can be well explained by using the analytic study presented in Appendix B. There, we model the density jump formed in our simulations with a simple functional form, and evaluate the net Lindblad torque a planet would feel. The results are shown in Fig. 13 and 14 for various density jumps and widths.

The surface mass density evolution for an Earth mass planet is exactly the same as Fig. 1, since the planet is totally embedded in a disk, and does not open a gap. From the left panel of Fig. 1, we can see the density jump is roughly two orders of magnitude at  $\sim 13$  AU, which spans about two pressure scale heights (here, the disk aspect ratio is  $h/r \sim 0.05$ ).

The rightmost panels of the middle row in Fig. 13 and 14 correspond to our simulations (a density jump  $F = 100$ , and a jump width  $\omega = 2h$ ). These figures suggest that such planets will feel a net positive torque (i.e. experience the outward migration) at a radius larger than  $r_{\text{edge}}/r_p = 0.8$  and  $0.7$  (or equivalently, less than 16.2 AU or 18.6 AU) respectively. Since the planet reverses its migration at  $\sim 18.3$  AU in Fig. 3, these analytical estimates are in good agreement with the numerical simulations.

Similarly, from the right panel, we see that the density jump is even larger at later times of the simulation ( $10^6 - 10^7$  years) — by about three orders of magnitude. Therefore, the planet feels a stronger torque than compared to the estimates in Fig. 13 and 14, and its orbit reaches the equilibrium at around 19.8 AU, where the inner and outer torques balance. This is the reason why we find the planet first halting its inward migration, and subsequently actually migrating some distance outward.

We next turn to the results for the migration of a  $10M_E$  planet. The left panel of Fig. 4 shows its migration in a disk *without* a dead zone. Again, it is clear that the planet plunges into the central star within  $1.5 \times 10^5$  years, which agrees well with the theory ( $\sim 10^5$  years).

The right panel of Fig. 4 shows the result of a similar simulation for a disk *with* a dead zone. This run follows a ten Earth mass planet that starts migrating from 20 AU. Again, the planet is repelled by the mass accumulation at the edge of the dead zone and starts migrating outward at  $\sim 16.5$  AU, which agrees well with the above estimate that is based on the analytical study in Appendix B. Before the 10 Earth mass planet gets repelled by the mass increase inside the dead zone, it migrates closer to the dead zone than the Earth mass planet does. This is because more massive planets migrate faster and hence get closer to the central star before the mass accumulation starts affecting their migration. Similar to the 1 Earth mass case, the planet stops migrating after it gets far from the surface mass density jump, at around  $\sim 19.5$  AU. Again, this result was checked until it converges by using smaller radial steps.

The left panel of Fig. 5 shows the migration of a  $1 M_J$  planet in disks *without* a dead

zone. We can see that the planet plunges into the star within  $5 \times 10^5$  years. This migration time roughly corresponds to the one expected from the theory ( $\sim 10^6$  years).

The right panel of Fig. 5 is the similar figure for a disk *with* a dead zone. Once again, we place a Jupiter mass planet in an initial orbit of 20 AU, just outside the outer dead zone radius (13 AU). Here, the planet migrates into the dead zone as it opens a gap, and drastically slows down its migration by the time it gets to 7 AU. The planet is not stopped by the surface density increase in the dead zone because it is locked into a clean disk gap, and is thus constrained to move along with the accretion flow of gas through the inner disk.

#### 4. Planet migration from inside the dead zone

Here, we will focus on the migration of planets whose initial orbits are within the dead zone. Intuitively, type I migration of planets inside the dead zones won't be affected by the existence of dead zones, since the type I migration does not depend on the disk's viscosity. However, as we have seen in §2.3, the gap-opening mass becomes smaller as the disk's viscosity decreases. Therefore, we expect that when the planetary mass is as large as  $M_E$  or  $10M_E$ , a planet inside a dead zone does not migrate straight into the central stars as it would in a disk without a dead zone. Instead, the planet ought to open a gap and thus slow down its migration significantly. This is partly because the fast type I migration is switched to the slower type II migration, and partly because the type II migration speed itself is slower inside the dead zones due to the lower viscosity there.

##### 4.1. Hybrid numerical simulations of planetary migration inside the dead zone

Fig. 6 shows the evolution of the same disk as the right panel of Fig. 3, and a 1 Earth mass planet starts migrating from 11 AU, just inside the outer dead zone radius (13 AU). Here, planet migration appears to be much faster than in a disk with no dead zone (left panel of Fig. 3). This is not surprising if we recall that the type I migration speed is proportional to the surface mass density (see Eq. 2). Due to a faster mass accretion from an active outer disk, the surface mass density inside the dead zone increases, which leads to faster migration. Also note that we cut the planet migration at  $\sim 1$  AU, due to the lower numerical resolution there, and that the planet is expected to open a gap within 1 AU from Fig. 2.

Fig. 7 shows the evolution of the same disk as the right panel of Fig. 4, and a 10 Earth mass planet starts migrating from 11 AU. Here, we find that the planet migrates in quickly, and opens a gap at around 4 AU. Note that, as expected from Rafikov (2002), the

center of the gap lags behind the migrating planet. Although the effect of the density wave propagation suggested by him is not included in our case, the physics is essentially the same. The density deficit that is formed in front of the planet is refilled by migration, but that behind the planet is not. The type I migration speed is faster than the left panel of Fig. 4 (a  $10 M_E$  planet migration in a disk with no dead zone) for the same reason as an  $M_E$  planet; the surface mass density increases inside the dead zone, which leads to the faster planetary migration (see Eq. 2). After a gap-opening, its migration speed drastically slows as expected. The gap-opening radius ( $\sim 4$  AU) agrees well with the theoretical estimate read from Fig. 2 ( $\sim 5$  AU). The gap-opening mass for such a low-mass planet can be estimated from the damping length of density waves (Rafikov 2002):

$$w \sim l_{\text{damping}} = 1.4 \left(\frac{2}{3}\right)^{7/5} \left(\frac{M_p}{M_*}\right)^{-2/5} \left(\frac{h}{r}\right)^{11/5} r. \quad (6)$$

The estimated gap-width of about 0.37 AU agrees well with the simulation ( $w \sim 0.4$  AU), although it should be pointed out that the damping of density waves is not included in our simulation.

Fig. 8 shows the evolution of the same disk as the right panel of Fig. 5, and a 1 Jupiter mass planet starts migrating from 11 AU. The planet migrates inward as it opens a gap, and significantly slows its migration inside the dead zone around 7 AU. This shows that the dead zone slows down the type II migration significantly. For a massive planet like Jupiter, the excited density waves shock and damp immediately, so we can estimate the gap width by equating the tidal torque  $T_{\text{tidal}} \sim C (r/w)^3 \Sigma r^2 (r\Omega)^2 (M_p/M_*)^2$  ( $C = 0.23$  in Lin & Papaloizou (1993)) with the viscous torque  $T_{\text{viscous}}$ :

$$\frac{w}{r} \sim \left(\frac{3\pi\alpha}{C}\right)^{-1/3} \left(\frac{r M_p}{h M_*}\right)^{2/3}. \quad (7)$$

In Fig. 9, we plot the calculated gap width for a Jupiter mass planet in a disk with  $\alpha = 10^{-5}$  (dashed and dotted lines,  $C = 1$  and  $0.23$  in Eq. 7 respectively) as well as the gap width determined from Fig. 8 (solid line). The planet starts migrating from 11 AU, and immediately opens a gap whose size is comparable to the analytical estimates. For example, from Fig. 8, we can see that 1 Jupiter mass planet inside the dead zone with a viscosity alpha parameter  $\alpha = 10^{-5}$  forms a gap of width  $\sim 4$  AU, which is comparable to its orbital radius, while the analytically calculated gap size is  $\sim 3.5$  AU at an orbital radius of 4 AU, which roughly agrees with the value we got.

## 5. Dependence upon Disk Viscosity Parameter: from Jupiter to hot Jupiters

Since there may be a significant range in values of the viscosity parameter  $\alpha$  across the entire ensemble of observed protostellar disks, we show a few other simulations with different values of  $\alpha$  here.

In Fig. 10, we show the Jupiter mass planet migration (type II migration) in a disk with  $\alpha = 10^{-5}$  inside the dead zone and  $\alpha = 10^{-3}$  outside it. Similar to the right panel of Fig. 5, the Jupiter mass planet migrates into the dead zone as it opens a gap, and slows down its migration significantly. After  $10^7$  years, the orbital radius of the planet is  $\sim 7$  AU.

In Fig. 11, we show the Jupiter mass planet migration in a disk with  $\alpha = 10^{-4}$  inside the dead zone and  $\alpha = 10^{-2}$  outside it. It is difficult to see from the figure, but the planet starts opening a gap *before* it enters the dead zone, at around 17 AU. The Jupiter mass planet migrates into the dead zone as it opens a gap, and slows down its migration. Due to the higher viscosity inside the dead zone, the migration is not slowed as much as Fig. 5 and 10. The final radius of the planet is  $\sim 0.1$  AU. Such planets may be good candidates for hot Jupiters. In our fiducial disk, the dead zone expands roughly between 0.04 and 13 AU. If a planet migrates further in, it could be stopped by the inner edge of the dead zone as suggested by Masset et al. (2006).

In Fig. 12, we show the Jupiter mass planet migration in a disk with  $\alpha = 10^{-4}$  inside the dead zone and  $\alpha = 10^{-3}$  outside it. Similar to the previous cases, the Jupiter mass planet migrates into the dead zone as it opens a gap, and slows down its migration. The migration inside the dead zone is faster than Fig. 5 and 10, but slower than Fig. 11. This is because the planet opens a wider gap long before the planet in Fig. 11 does, and thus slows down earlier. After  $10^7$  years, the orbital radius of the planet is  $\sim 3.5$  AU.

These simulations indicate that planet migration is very sensitive to the disk’s viscosity, and that dead zones with  $\alpha = 10^{-4} - 10^{-5}$  can place planets anywhere between  $\sim 0.1$  and  $\sim 7$  AU. In other words, just by changing the viscosity parameter inside the dead zone by one order of magnitude we could get our Jupiter like planet (Fig. 5, 10, or 12) or a potential candidate for a hot Jupiter (Fig. 11).

## 6. Discussion and Conclusion

We have studied planet migration in disks with dead zones, and compared the results with the migration in disks with no dead zones. Specifically, we studied the evolution of planets of mass  $M_E$ ,  $10M_E$ , and  $M_J$ , which are initially placed in orbits both in well coupled,

magnetically active, and hence viscous regions as well as inside the dead zone.

Throughout, we have only considered planets on circular orbits. In the case of type I migration, this is a reasonable assumption. Planets are subject to strong eccentricity damping, on an even much shorter timescale than the orbital decay (e.g. Artymowicz 1993; Papaloizou & Larwood 2000), and therefore core-sized bodies are likely to spend almost all their time with very low eccentricities. Damping becomes weaker once a gap opens (i.e. in type II regime). In fact, the disk-planet interaction for a gap-opening planet could lead to eccentricity enhancement (e.g. Artymowicz 1993; Goldreich & Sari 2003), but the issue of gas giant eccentricities is beyond the scope of this work.

For planets migrating toward the dead zone in the active part of the disk, there are some issues that we have not explicitly calculated. First of all, as we have already mentioned, we have not included the effect of the corotation torque. This is potentially important when planets are migrating toward the density jump generated by a dead zone. If the corotation torque is stronger than the Lindblad torque, planets would be brought into the dead zone instead of being repelled. However, we showed that this is unlikely from the results of Appendix B. For steep density cases relevant to our simulations, Fig. 13 and 14 show that the Lindblad torque changes the sign from negative to positive at  $0.7 \lesssim r_{\text{edge}}/r_p \lesssim 0.8$  (see panels with a density jump  $F = 100$ , and a jump width  $\omega \sim h - 2h$ ). Therefore, the net Lindblad torque forces a planet to migrate *outward* at several pressure scale heights away from the dead zone edge. This can be easily seen by noting  $5 \lesssim (r_p - r_{\text{edge}})/h_{\text{edge}} \lesssim 8.6$  with  $r_{\text{edge}} = r_{DZ} = 13$  AU and  $h_{\text{edge}}/r_{\text{edge}} \sim 0.05$ . Since the corotation torque has a significant effect on a length scale of the density jump width, our results ensure that the Lindblad torque starts acting on a planet *before* the corotation torque becomes effective. Even if the corotation torque becomes comparable to the Lindblad torque, it is unlikely the former exceeds the latter. This is because the magnitude of the net Lindblad torque close to the density jump (positive torque) is much larger than that of the original Lindblad torque far from the jump (negative torque).

Secondly, turbulent fluctuations in active disk may cause corresponding fluctuations in the torque felt by a planet during type I migration (Laughlin et al. 2004; Nelson & Papaloizou 2004; Nelson 2005; Johnson et al. 2006). In principal, if such fluctuations are large enough, this may make it possible for planets/cores to “jump the barrier” provided by the edge of a dead zone, instead of being repelled by it. Such behavior can be expected if the density fluctuations,  $\delta\Sigma/\Sigma$ , become comparable to the density jump between active and dead zone. When this happens, the planets would migrate just like the ones inside the dead zone, i.e. type I migrators open a gap, and slow their migration as seen in §4.

Thirdly, in our simulations a density jump becomes steep enough so that the disk is

locally Rayleigh unstable ( $\kappa^2 < 0$ , see Appendix B for the expression). This will smooth out the density contrast to some degree. Therefore, a density jump in a more realistic disk would not be as steep as our models. This could affect the migration starting from outside the dead zone — a planet may not be reflected as strongly as we have shown. We leave an investigation of this issue to future work.

In all three of these instances, we see that although the details of the migration will change, the dead zone will still provide an effective barrier through the onset of type II migration.

We list the conclusions of our paper below:

(i) Type II migration can be significantly slowed down inside the dead zones (see §3 and 4). This is because the type II migration speed is directly proportional to the disk’s viscosity, and because the dead zones are expected to have a very low viscosity. Jupiter mass planets open a gap inside dead zones and almost stop their migration at around 4 – 8 AU when the viscosity parameter is  $\alpha = 10^{-5}$ .

(ii) Type I migrators are stopped at the edge of the dead zone (see §3, as well as Fig. 3 and 4). This is because type I migration depends on the difference between inner and outer torque strengths. Due to the mass accumulation at the edge of the dead zone, the magnitude of the inner torque becomes larger as a planet approaches the edge, eventually canceling the outer torque. This mechanism leaves both 1 Earth and 10 Earth mass planets at  $\sim 20$  AU at early times, though they would move inward as the dead zone contracts over time.

(iii) Type I migration inside the dead zone can be changed to a slower type II migration (see §4, as well as Fig. 7). Type I migration itself won’t be slowed down by the presence of the dead zones, since the migration speed does not depend on the disk’s viscosity. The gap-opening masses, however, become much smaller inside the dead zones, and therefore even small mass planets (e.g.  $M_E$  and  $10M_E$ ) can open a gap there. Although we assume that density waves damp immediately, and hence do not include the wave damping effect proposed by Rafikov (2002), our simulations show that a 10 Earth mass planet may open a gap at  $\sim 4$  AU, which slows down its migration dramatically.

(iv) We also showed that the analytically calculated gap-width agrees well with the results of simulations (see §4, as well as Fig. 9).



(v) The dependence of migration on the viscosity parameter is significant. If the viscosity outside the dead zone is measured with  $\alpha \sim 10^{-2} - 10^{-3}$ , our simulations indicate that, after  $10^7$  years, the orbital radius of planets could vary from our Jupiter-like orbital radius  $\sim 3.5 - 7$  AU (see Fig. 5, 10, and 12) to hot Jupiter-like radius  $\sim 0.1$  AU (Fig. 11).

Our approach so far has ignored the evolution of the dead zone which arises from the accretion of their surface layers onto the central star. We also ignored the fact that planets accrete a significant fraction of their mass while they migrate. We will study planetary accretion during migration in a disk with an evolving dead zone in our next paper.

We thank an anonymous referee for useful comments on our manuscript. S. M. is supported by McMaster University, R. E. P. is supported by a grant from the National Sciences and Engineering Research Council of Canada (NSERC), and E. W. T. is supported by NSERC and CITA.

### A. The saturation of corotation resonance inside a dead zone

Here, we will discuss whether a gap-opening terrestrial mass planets inside a dead zone executes type III migration instead of type II migration.

The type III migration is driven by the corotation torque, which is proportional to the inverse of vortensity gradient ( $d \ln(\Sigma/B)/d \ln r$ ) (e.g. Goldreich & Tremaine 1980). This gradient, however, tends to be removed due to the libration of co-orbital material, and therefore the corotation torque saturates, unless the gradient is re-established by viscous torque (e.g. Ward 1992; Masset 2001). The corotation torque will not saturate if the horseshoe libration timescale ( $t_{HS} \sim 4\pi r_p/(1.5\Omega_p x_s)$ ) is longer than the viscous timescale ( $t_{viscous} \sim x_s^2/(3\nu)$ ) (Masset & Papaloizou 2003):

$$\alpha > \frac{1}{8\pi} \left( \frac{M_p}{M_*} \right)^{3/2} \left( \frac{h_p}{r_p} \right)^{-7/2}, \quad (\text{A1})$$

where the horseshoe zone half-width is taken to be  $x_s = 0.96r_p\sqrt{(M_p r_p)/(M_* h_p)}$ , following Masset & Papaloizou (2003).

Since the gap-opening mass for low mass planets like  $M_E$  or  $10M_E$  in a gravitationally stable, low viscosity disk ( $\alpha \sim 10^{-5}$ ) is well approximated by Eq. 5, we replace the mass

ratio in the above equation with this, and obtain the following relation:

$$\alpha > 8.66 \times 10^{-4} \left( \frac{h_p/r_p}{0.04} \right) \left( \min \left[ 0.301 \left( \frac{Q}{54} \right)^{-5/7}, 0.237 \left( \frac{Q}{54} \frac{0.04}{h_p/r_p} \right)^{-5/13} \right] \right)^{3/2}, \quad (\text{A2})$$

where  $Q = 54$  and  $h/r = 0.04$  are values estimated at 1 AU in our fiducial disk. Here, the last term in the round bracket is of the order of  $\sim 0.115$ , and hence  $\alpha \gtrsim 10^{-4}$  is needed to prevent the saturation of corotation torque. Therefore, it is arguable whether the corotation torque plays a significant role for planets migrating inside a dead zone, where the viscosity parameter is very small ( $\alpha = 10^{-4} - 10^{-5}$ ).

## B. Type I migration toward a density jump — the effect of Lindblad torque

Here, we wish to investigate the effect of a jump in azimuthally-averaged gas disk surface density on the gravitational torques experienced by embedded non-gap opening (i.e. Type I) bodies. We introduce an artificial jump into a power-law surface density profile as follows:

$$\Sigma = \Sigma_{\text{base}} + (F - 1)\Sigma_{\text{base}} \left[ \frac{1}{2} - \frac{1}{2} \tanh \left( \frac{r - r_{\text{edge}}}{\omega} \right) \right], \quad (\text{B1})$$

which is a good approximation of the density jump seen in our simulations, for example, Fig. 1. Thus we have a surface density which, going from large to small  $r$ , rises smoothly by a factor  $F$  over a radial distance  $\omega$ , centered on  $r = r_{\text{edge}}$ . The radial pressure gradient in the disk causes the azimuthal frequency to differ from their Keplerian values:

$$\Omega^2(r) = \frac{GM_*}{r^3} + \frac{1}{r\rho} \frac{\partial}{\partial r} (\rho c_s^2). \quad (\text{B2})$$

This then also has a direct effect on the epicyclic frequency since

$$\kappa^2(r) = \frac{1}{r^3} \frac{\partial}{\partial r} (r^4 \Omega^2). \quad (\text{B3})$$

Thus, at locations of steep density gradients, these frequencies can be significantly non-Keplerian.

A planet on a circular orbit in a protostellar disk acts as a perturbation potential of the disk and exerts torques at the vicinity of the Lindblad resonances, which lead to the transfer of angular momentum. The perturbation potential can be expanded into a Fourier series, and the torque around an  $m$ th order resonance,  $T_{\text{tidal},m}$ , can be expressed in terms of the amplitude of the potential of a corresponding order (Goldreich & Tremaine 1980). The

planet-disk interaction is calculated through the average torque per radial step (i.e. torque density  $dT_{\text{tidal}}/dr$ ) as can be seen in Eq. 1. Assuming the angular momentum transfer is smooth (i.e. the damping distance of the waves is longer than the distance between resonances), a smooth torque density can be written as (Ward 1997):

$$\frac{dT_{\text{tidal}}}{dr} = T_{\text{tidal},m} \left| \frac{dm}{dr} \right|. \quad (\text{B4})$$

Following the formulation of Ward (1997) (see also Menou & Goodman 2004), the smooth torque density experienced by the disk due to a planet of mass  $M_p = \mu M_*$  on a circular orbit about a primary of mass  $M_*$  at radius  $r_p$ , is

$$\frac{dT_{\text{tidal}}}{dr}(r) = \text{sgn}(r - r_p) \frac{2\mu^2 \Sigma(r) r_p^4 \Omega_p^4}{r(1 + 4\xi^2) \kappa^2} m^4 \psi^2 \quad (\text{B5})$$

where  $\xi \equiv mc_s/r\kappa$  measures the change to the Lindblad resonances due to finite gas pressure,  $c_s$  is the gas sound speed, and  $\psi$  is the dimensionless forcing function due to a planet's potential that is written as:

$$\psi = \frac{\pi}{2} \left[ \frac{1}{m} \left| \frac{db_{1/2}^m}{d\beta} \right| + 2 \frac{\Omega}{\kappa} \sqrt{1 + \xi^2} b_{1/2}^m(\beta) \right], \quad (\text{B6})$$

with  $\beta \equiv r/r_p$  and  $b_{1/2}^m(\beta)$  being the Laplace coefficient:

$$b_{1/2}^m(\beta) \equiv \frac{2}{\pi} \int_0^\pi \frac{\cos m\theta d\theta}{\sqrt{1 - 2\beta \cos \theta + \beta^2}}. \quad (\text{B7})$$

The largest contribution to the integral above comes from  $\theta \ll 1$ , and it can be well approximated by the modified Bessel function of the second kind of order 0,  $K_0(z)$ , which decays exponentially for  $z \gg 1$  (Goldreich & Tremaine 1980; Menou & Goodman 2004).

To take account of the 3D torque effect (i.e. effect of the finite thickness of the disk) in a simple approximate way, we followed Menou & Goodman (2004) with a softened approximation,

$$b_{1/2}^m(\beta) \approx \frac{2}{\pi\beta^{1/2}} K_0 \left( m \sqrt{\beta - 2 + \frac{1}{\beta} + \frac{(Bh)^2}{rr_p}} \right) \quad (\text{B8})$$

with  $h \approx c_s/\Omega$  the disk scale height, and  $B$  a dimensionless scaling factor parameterizing the softening in units of the disk scale height. Therefore, although the hybrid code calculates a 1D disk evolution, the interaction between the disks and planets is evaluated by using an approximated 3D torque density. In going from a summation of torques at discrete

resonances to a torque density, the wavenumber  $m$  is turned into a continuous function of radius:

$$m(r) = \left[ \frac{\kappa^2}{(\Omega - \Omega_p)^2 - c_s^2/r^2} \right]^{1/2}. \quad (\text{B9})$$

Using Eq. B1 for the surface density, we numerically compute the summed torque from Eq. B5 in Matlab. We normalize the torque as in Ward (1997), dividing by a reference torque

$$\tau_0 = \mu^2 \left( \frac{\pi r_p^2 \Sigma_p}{M_*} \right) M_*(r_p \Omega_p)^2 \left( \frac{r_p}{h_p} \right)^3, \quad (\text{B10})$$

where the subscript  $p$  denotes a quantity evaluated at  $r = r_p$ .

We begin by adopting  $B = 0$ , i.e. the torques are calculated two-dimensionally. Fig. 13 shows the normalized total torque computed as a function of  $r_{\text{edge}}/r_p$ , for different values of density jump height  $F$  and width  $\omega$ . The width is in units of the disk scale height  $h$  at  $r = r_{\text{edge}}$ . The base surface density is a power law,  $\Sigma_{\text{base}} \propto r^{-3/2}$ , as is the sound speed,  $c_s \propto r^{-1/4}$ . While the planet is still far from the density jump, the net torque is negative and approximately constant with  $r_{\text{edge}}/r_p$ . When the surface density jumps by a factor  $F = 5$  or 10 over a radial distance of  $4h$ , the net torque on the planet is always negative, no matter where inside its orbit the density jump occurs. However, when the density jumps by a factor of 100 over  $4h$ , the net torque becomes positive when  $r_{\text{edge}} \approx 0.75r_p$ . Though  $\tau_{\text{net}}$  becomes negative again for slightly larger  $r_{\text{edge}}$ , a body migrating toward the edge will stop where  $\tau_{\text{net}}$  first becomes zero, and get hung up there. In this way, a jump in the azimuthally-averaged gas disk surface density can completely stop Type I migration.

Note that decrease/fluctuations in  $\tau_{\text{net}}$  for  $r_{\text{edge}} > 0.75r_p$  result because the region of highest torque density close to the planet is beginning to overlap the region of the density jump. In reality, this close to the jump, corotation torques would start to dominate over Lindblad torques, so our calculation of  $\tau_{\text{net}}$  is any case no longer valid here. Also, it should be pointed out that the steepest jump ( $F = 100$ ,  $\omega = h$  over a distance  $h$ ) actually produces a locally imaginary epicyclic frequency and as such would be subject to Rayleigh instability. This would reduce the density jump, which may even change the migration direction. We leave this investigation to future work.

Further examination of the remaining panels of Fig. 13 reveals that when the density jump occurs over  $2h$  or  $h$ , the torque eventually becomes positive no matter whether the density jumps by a factor of 100, 10 or even 5. The exact value of  $r_{\text{edge}}/r_p$  at which this happens changes, but in all cases, it is greater than the half-width of the jump,  $(\omega/2)/r_p$ . In other words, the net torque becomes zero before the density jump itself reaches the planet's orbital radius. This is important because once a planet finds itself at the same radius as

the density jump, the corotation torques responsible for type III migration (see §1), not included in this calculation, may overpower the Lindblad torques, with the effect being in the opposite sense: the planet is pulled *toward* the higher-density region (Masset et al. 2006). However, when the Lindblad torque switches from negative to positive at a significant standoff distance from the density jump already, approaching planets will be stopped while the corotation torques are still small compared to the Lindblad torques. Furthermore, for all cases with density jumps over a distance  $h$ , as well as over  $2h$  with a  $100 \times$  jump, the magnitude of the largest positive torque exceeds that of the negative torque. This ensures that even if the corotation torque becomes comparable to the Lindblad torque, the planet will still be stopped in these cases.

We repeat the calculation with a vertically-softened torque,  $B = 0.5$ . As shown by Menou & Goodman (2004), this “pseudo-3D” torque introduces two major differences relative to the 2D calculation above. First, the torque asymmetry becomes smaller because the strong contribution from the parts of the disk near the planet, just outside of the torque cutoff, are weakened. Second, the dependence of the net torque on the steepness of the disk surface density changes qualitatively. In the 2D case, in a smooth power-law disk, the net normalized torque is almost independent of the power law index. However, with softening, the torque asymmetry becomes weaker as the surface density becomes steeper. Both of these effects ought to conspire to make density jumps even more effective at arresting Type I migration.

The results of the calculation are shown in Fig. 14. Indeed, the effect of the surface density jumps on migration is even stronger than in the 2D case above. Now, every combination of  $F = 5, 10, 100$  and  $\omega = h, 2h, 4h$  results in  $\tau_{\text{net}}$  becoming positive as  $r_{\text{edge}}$  approaches  $r_p$ , and in each case this happens at a somewhat smaller value of  $r_{\text{edge}}/r_p$  than in the corresponding 2D calculation. In other words, the migrating planet is stopped at a slightly greater standoff distance from the density jump. Also, all combinations except  $F = 5$  with  $\omega = 4h$  result in the positive torque far exceeding the original negative torque well before the planet reaches the density transition region, thus ensuring that corotation torques cannot play a significant role.

## REFERENCES

- Alibert, Y., Mordasini, C., Benz, W., & Winisdoerffer, C. 2005, *A&A*, 434, 343
- Artymowicz, P. 1993, *ApJ*, 419, 166

- Artymowicz, P. 2004, in ASP Conf. Ser. 324: Debris Disks and the Formation of Planets, ed. L. Caroff, L. J. Moon, D. Backman, & E. Praton, 39–+
- Balbus, S. A. & Hawley, J. F. 1991, *ApJ*, 376, 214
- Bryden, G., Chen, X., Lin, D. N. C., Nelson, R. P., & Papaloizou, J. C. B. 1999, *ApJ*, 514, 344
- Butler, R. P., Wright, J. T., Marcy, G. W., Fischer, D. A., Vogt, S. S., Tinney, C. G., Jones, H. R. A., Carter, B. D., Johnson, J. A., McCarthy, C., & Penny, A. J. 2006, *ApJ*, 646, 505
- Chiang, E. I., Joungh, M. K., Creech-Eakman, M. J., Qi, C., Kessler, J. E., Blake, G. A., & van Dishoeck, E. F. 2001, *ApJ*, 547, 1077
- Duncan, M. J., Levison, H. F., & Lee, M. H. 1998, *AJ*, 116, 2067
- Fleming, T. & Stone, J. M. 2003, *ApJ*, 585, 908
- Fromang, S., Terquem, C., & Balbus, S. A. 2002, *MNRAS*, 329, 18
- Gammie, C. F. 1996, *ApJ*, 457, 355
- Glassgold, A. E., Najita, J., & Igea, J. 1997, *ApJ*, 480, 344
- Goldreich, P. & Sari, R. 2003, *ApJ*, 585, 1024
- Goldreich, P. & Tremaine, S. 1979, *ApJ*, 233, 857
- . 1980, *ApJ*, 241, 425
- Johnson, E. T., Goodman, J., & Menou, K. 2006, *ApJ*, 647, 1413
- Laughlin, G., Steinacker, A., & Adams, F. C. 2004, *ApJ*, 608, 489
- Lecar, M., Podolak, M., Sasselov, D., & Chiang, E. 2006, *ApJ*, 640, 1115
- Lin, D. N. C., Bodenheimer, P., & Richardson, D. C. 1996, *Nature*, 380, 606
- Lin, D. N. C. & Papaloizou, J. C. B. 1993, *Protostars and Planets III* (The University of Arizona Press)
- Lineweaver, C. H. & Grether, D. 2003, *ApJ*, 598, 1350
- Marcy, G. W. & Butler, R. P. 1996, *ApJL*, 464, L147+

- Masset, F. S. 2001, *ApJ*, 558, 453
- Masset, F. S., Morbidelli, A., Crida, A., & Ferreira, J. 2006, *ApJ*, 642, 478
- Masset, F. S. & Papaloizou, J. C. B. 2003, *ApJ*, 588, 494
- Matsumura, S. & Pudritz, R. E. 2003, *ApJ*, 598, 645
- . 2005, *ApJL*, 618, L137
- . 2006, *MNRAS*, 365, 572
- Mayor, M. & Queloz, D. 1995, *Nature*, 378, 355
- Menou, K. & Goodman, J. 2004, *ApJ*, 606, 520
- Nelson, R. P. 2005, *A&A*, 443, 1067
- Nelson, R. P. & Papaloizou, J. C. B. 2004, *MNRAS*, 350, 849
- Papaloizou, J. C. B. & Larwood, J. D. 2000, *MNRAS*, 315, 823
- Pollack, J. B., Hubickyj, O., Bodenheimer, P., Lissauer, J. J., Podolak, M., & Greenzweig, Y. 1996, *Icarus*, 124, 62
- Pringle, J. E. 1981, *ARA&A*, 19, 137
- Rafikov, R. R. 2002, *ApJ*, 572, 566
- Robberto, M., Beckwith, S. V. W., & Panagia, N. 2002, *ApJ*, 578, 897
- Sano, T., Miyama, S. M., Umebayashi, T., & Nakano, T. 2000, *ApJ*, 543, 486
- Santos, N. C., Benz, W., & Mayor, M. 2005, *Science*, 310, 251
- Semenov, D., Wiebe, D., & Henning, T. 2004, *A&A*, 417, 93
- Shu, F., Najita, J., Ostriker, E., Wilkin, F., Ruden, S., & Lizano, S. 1994, *ApJ*, 429, 781
- Tanaka, H., Takeuchi, T., & Ward, W. R. 2002, *ApJ*, 565, 1257
- Terquem, C. E. J. M. L. J. 2003, *MNRAS*, 341, 1157
- Thommes, E. W. 2005, *ApJ*, 626, 1033
- Thommes, E. W. & Murray, N. 2006, *ApJ*, 644, 1214

Trilling, D. E., Benz, W., Guillot, T., Lunine, J. I., Hubbard, W. B., & Burrows, A. 1998, *ApJ*, 500, 428

Udry, S., Mayor, M., & Santos, N. C. 2003, *A&A*, 407, 369

Ward, W. R. 1992, in *Lunar and Planetary Institute Conference Abstracts*, 1491–+

Ward, W. R. 1997, *Icarus*, 126, 261

Wisdom, J. & Holman, M. 1991, *AJ*, 102, 1528



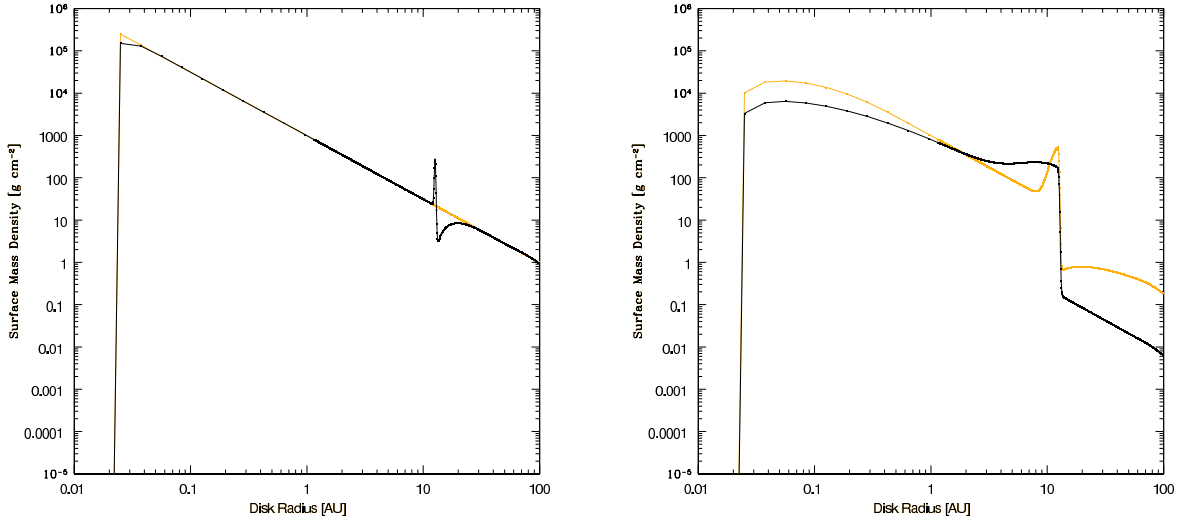


Fig. 1.— Left: The surface mass density evolution of a disk with a dead zone. The dead zone radius is fixed at 13 AU. The light-colored line is the initial power-law profile of the surface mass density, and the dark line is the density profile after  $10^4$  years. Right: The same for  $10^6$  years (light-colored line) and  $10^7$  (dark line) years. The surface mass density is gradually flattened due to the small viscosity inside the dead zone.

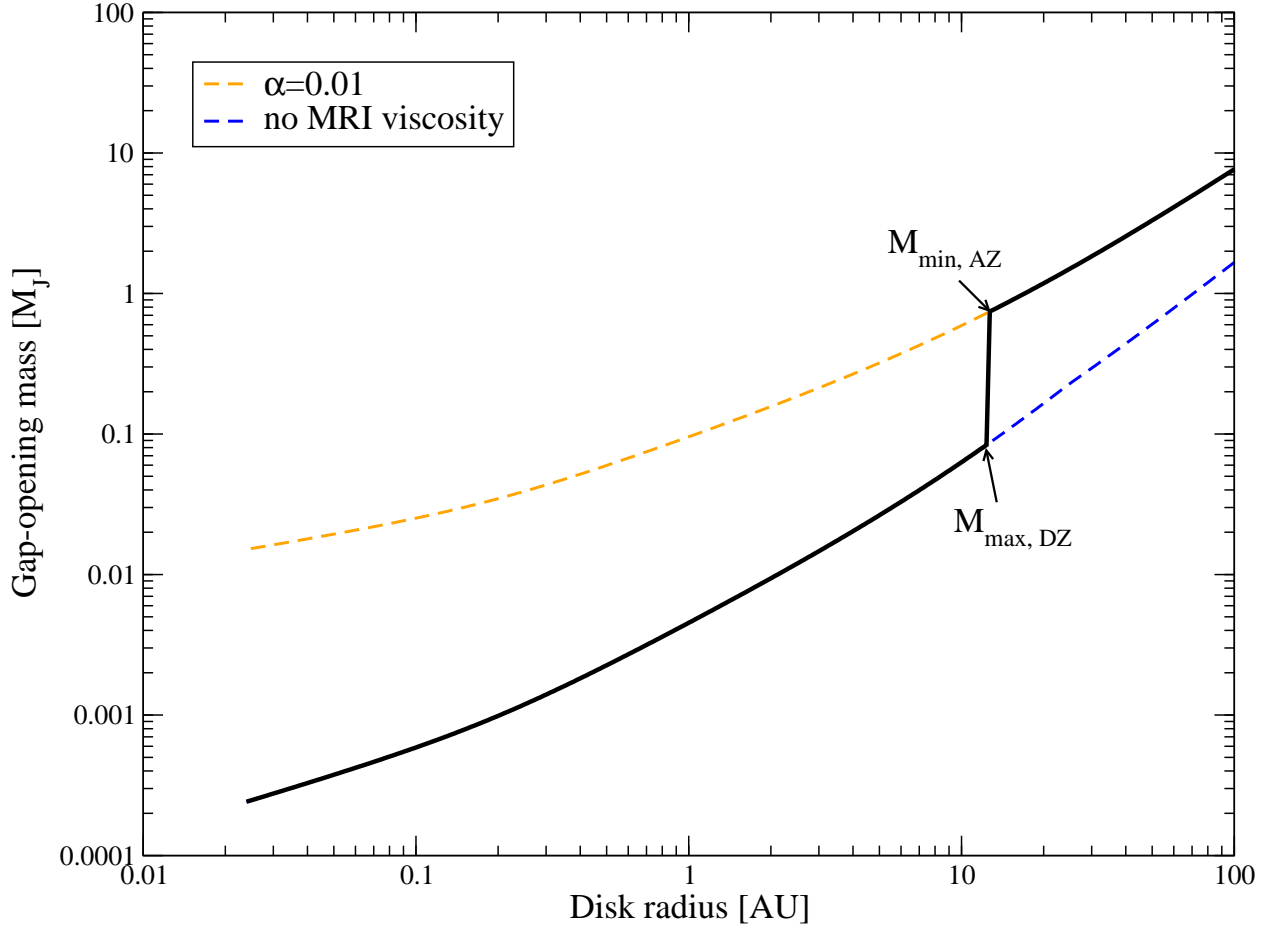


Fig. 2.— Gap-opening masses for a disk exposed to an external star which has the surface mass density, at 1 AU, of  $\Sigma_0 = 10^3 \text{ g cm}^{-2}$ . The lower dashed line shows the gap-opening mass for the case of no MRI viscosity, while the upper dashed line shows the gap-opening masses for  $\alpha_{ss} = 10^{-2}$ . For the magnetic Reynolds number  $Re_M = 10^3$ , the fiducial minimum gap-opening mass throughout the disk is shown in a solid line.

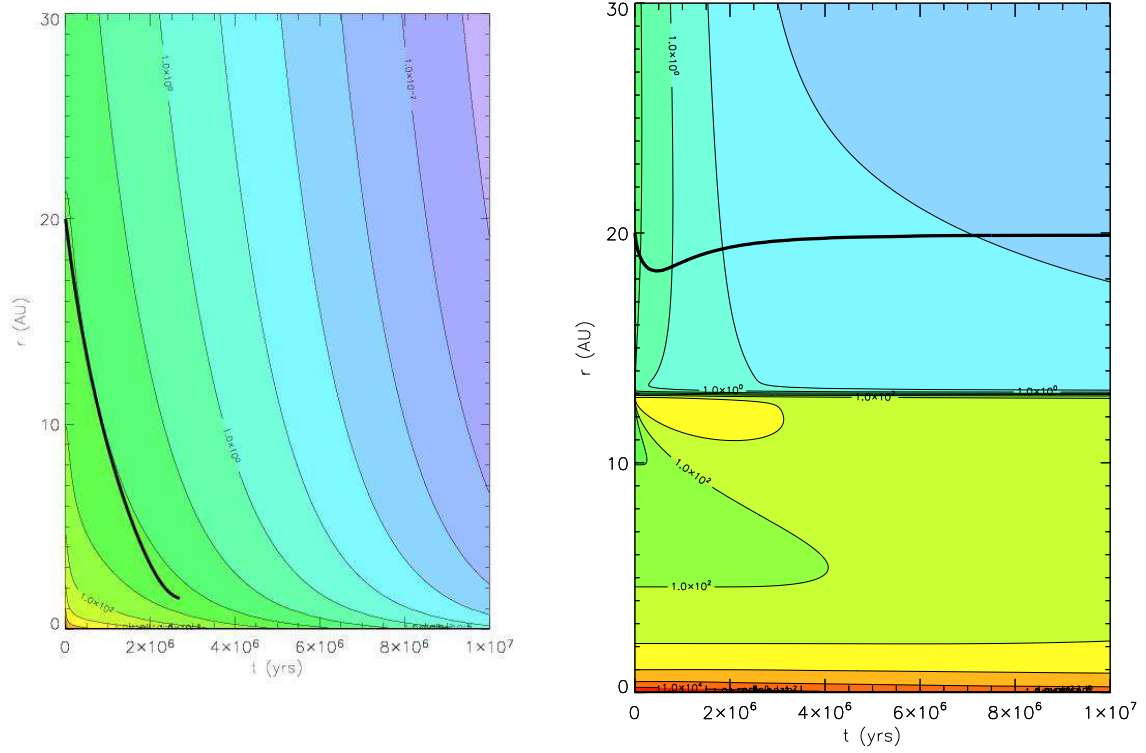


Fig. 3.— Left: Time evolution of the disk and planet without a dead zone. The trajectory of a  $1 M_E$  planet, initially at 20 AU, is shown in a heavy black line. Also shown is surface mass density contours which become denser from blue to red. The planet migrates down to  $\sim 1$  AU within  $3 \times 10^6$  years. Right: Time evolution of the 1D disk with a dead zone’s outer radius at 13 AU. The  $1 M_E$  planet migrates inward a bit, but then gets repelled by the mass accumulation at the edge of the dead zone and migrates out to  $\sim 19.8$  AU. Color figures are available on the web.

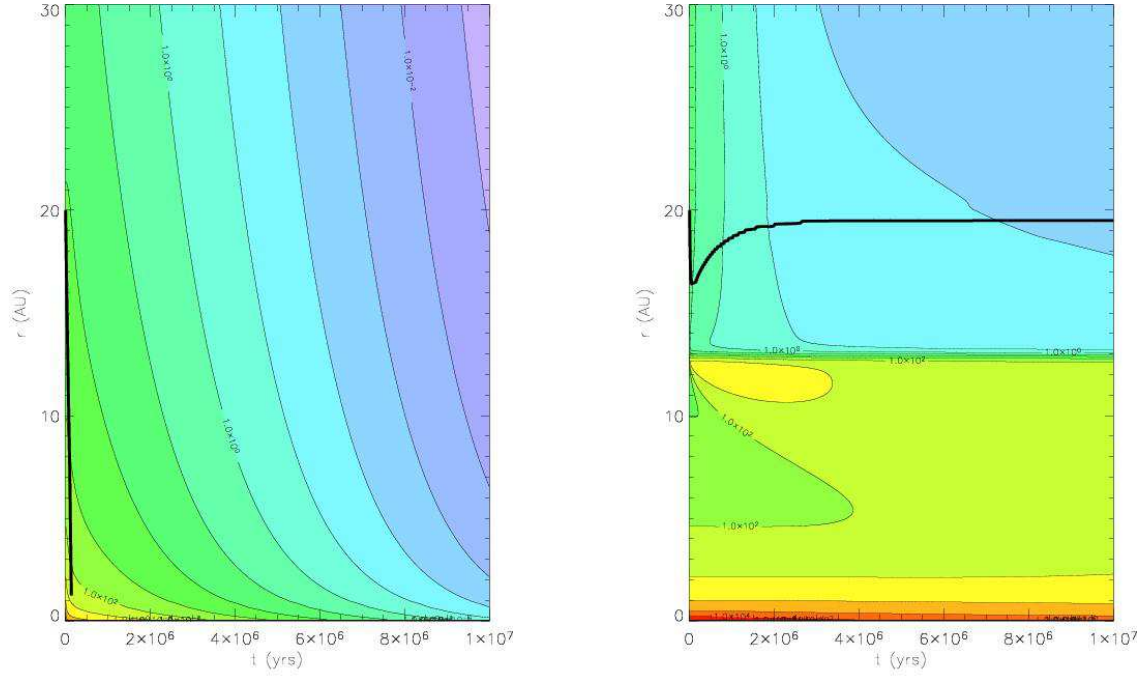


Fig. 4.— Left: Time evolution of the disk and planet without a dead zone. The trajectory of a  $10 M_E$  planet, initially at 20 AU, is shown in a heavy black line. Also shown is surface mass density contours which become denser from blue to red. The planet migrates down to  $\sim 1$  AU within  $1.5 \times 10^5$  years. Right: Time evolution of the 1D disk with a dead zone’s outer radius at 13 AU. The  $10 M_E$  planet migrates inward a bit, but then gets repelled by the mass accumulation at the edge of the dead zone and migrates out to  $\sim 19.5$  AU.

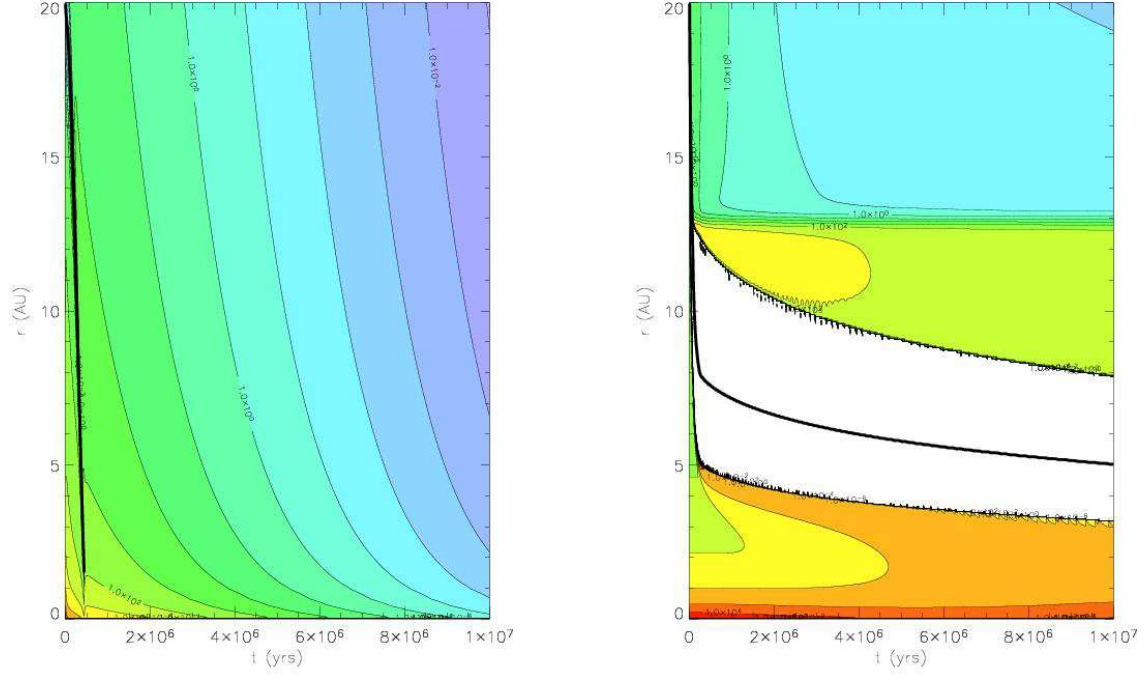


Fig. 5.— Left: Time evolution of the disk and planet without a dead zone. The trajectory of a  $1 M_J$  planet, initially at 20 AU, is shown in a heavy black line. Also shown is surface mass density contours which become denser from blue to red. The planet migrates inward as it opens a gap and plunges into the central star within half a million years. Right: Time evolution of the 1D disk with a dead zone’s outer radius at 13 AU. The  $1 M_J$  planet migrates inward as it opens a wide gap at around 6 AU. Its migration is significantly slowed down after the gap-opening.

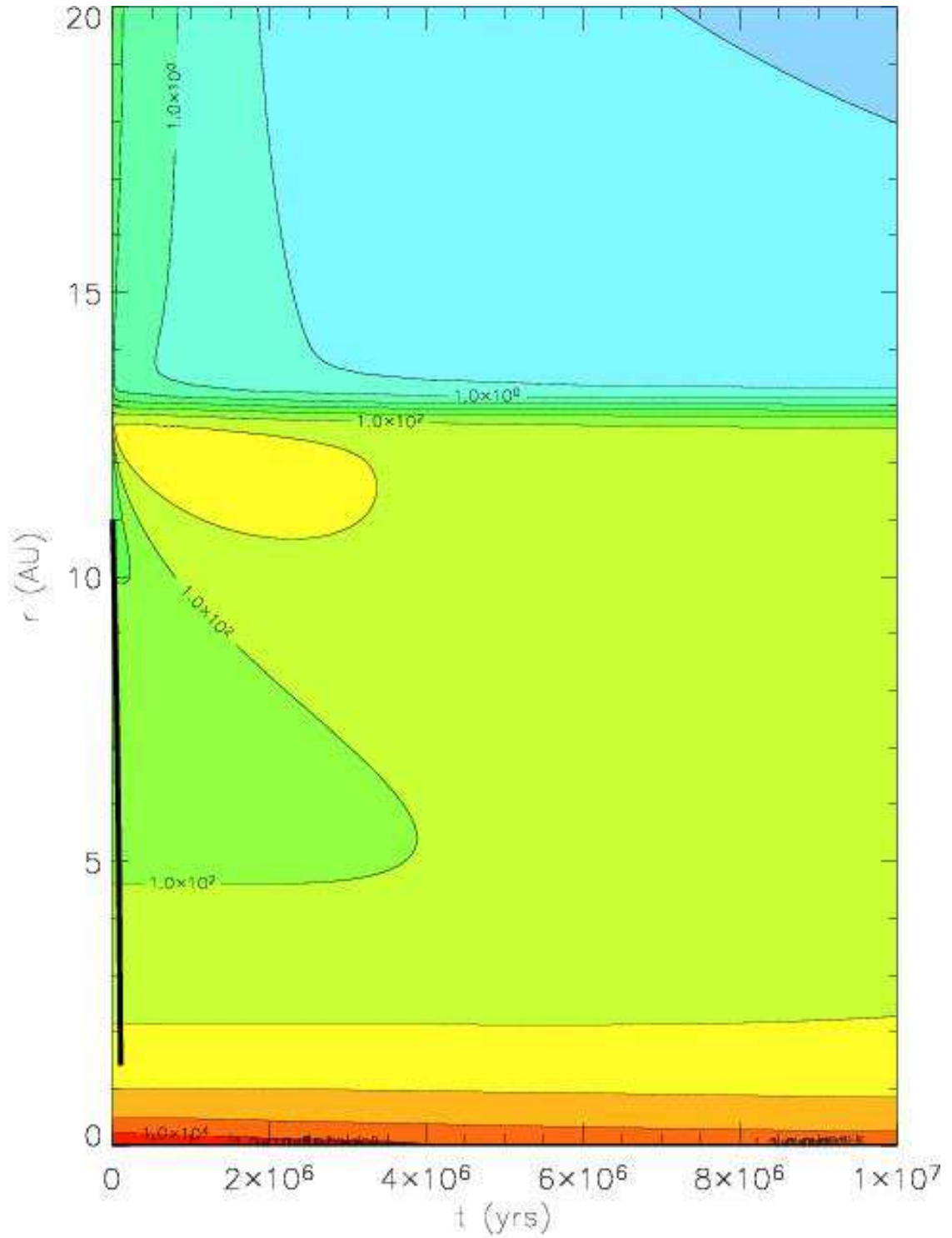


Fig. 6.— The same as Fig. 3, but the  $1 M_E$  planet starts migrating from just inside the dead zone, namely 11 AU. In this case, the type I migration becomes even faster inside the dead zone due to the increase in mass density. From Fig. 2, the planet is expected to open a gap around 0.7 AU, which is not shown here.

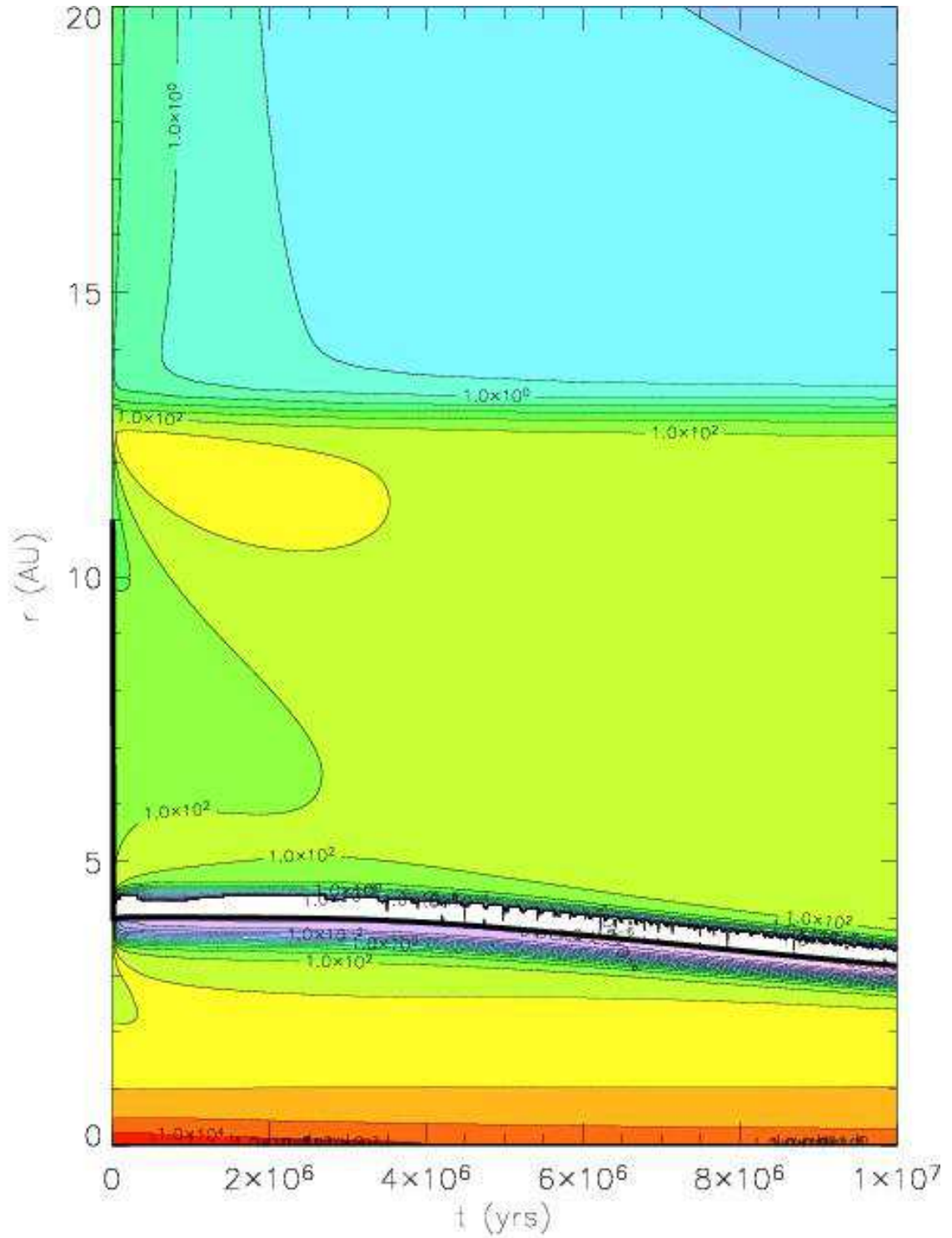


Fig. 7.— The same as Fig. 4, but the  $10 M_E$  planet starts migrating from just inside the dead zone, namely 11 AU. The planet migrates inward, and opens a gap at  $\sim 4$  AU, which agrees well with the estimate from Fig. 2 ( $\sim 5$  AU). After the gap-opening, its migration speed is significantly slowed down.

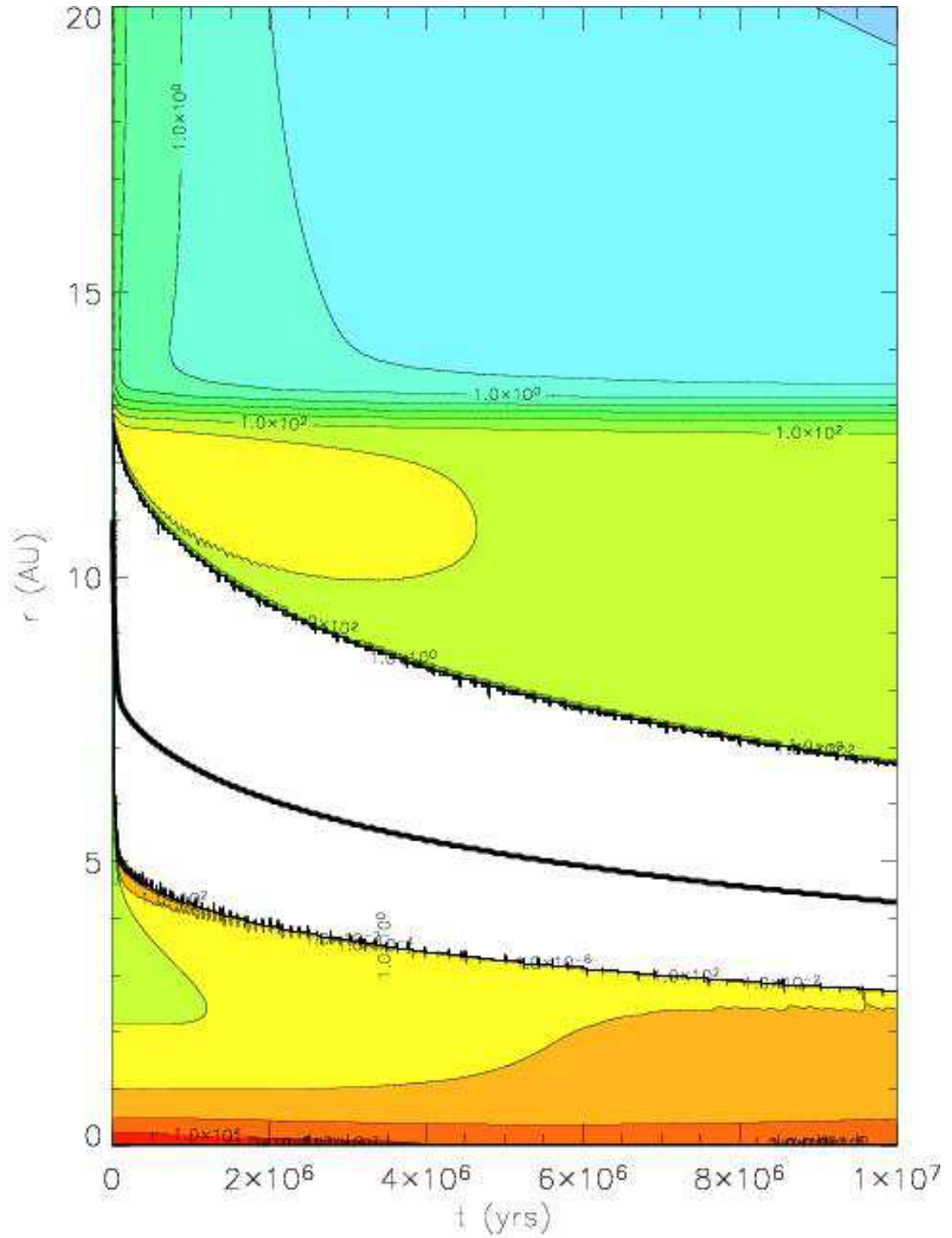


Fig. 8.— The same as Fig. 5, but the  $1 M_J$  planet starts migrating from just inside the dead zone, namely 11 AU. The planet migrates inward, and opens a gap at  $\sim 5$  AU. After the gap-opening, its migration speed is significantly slowed down.



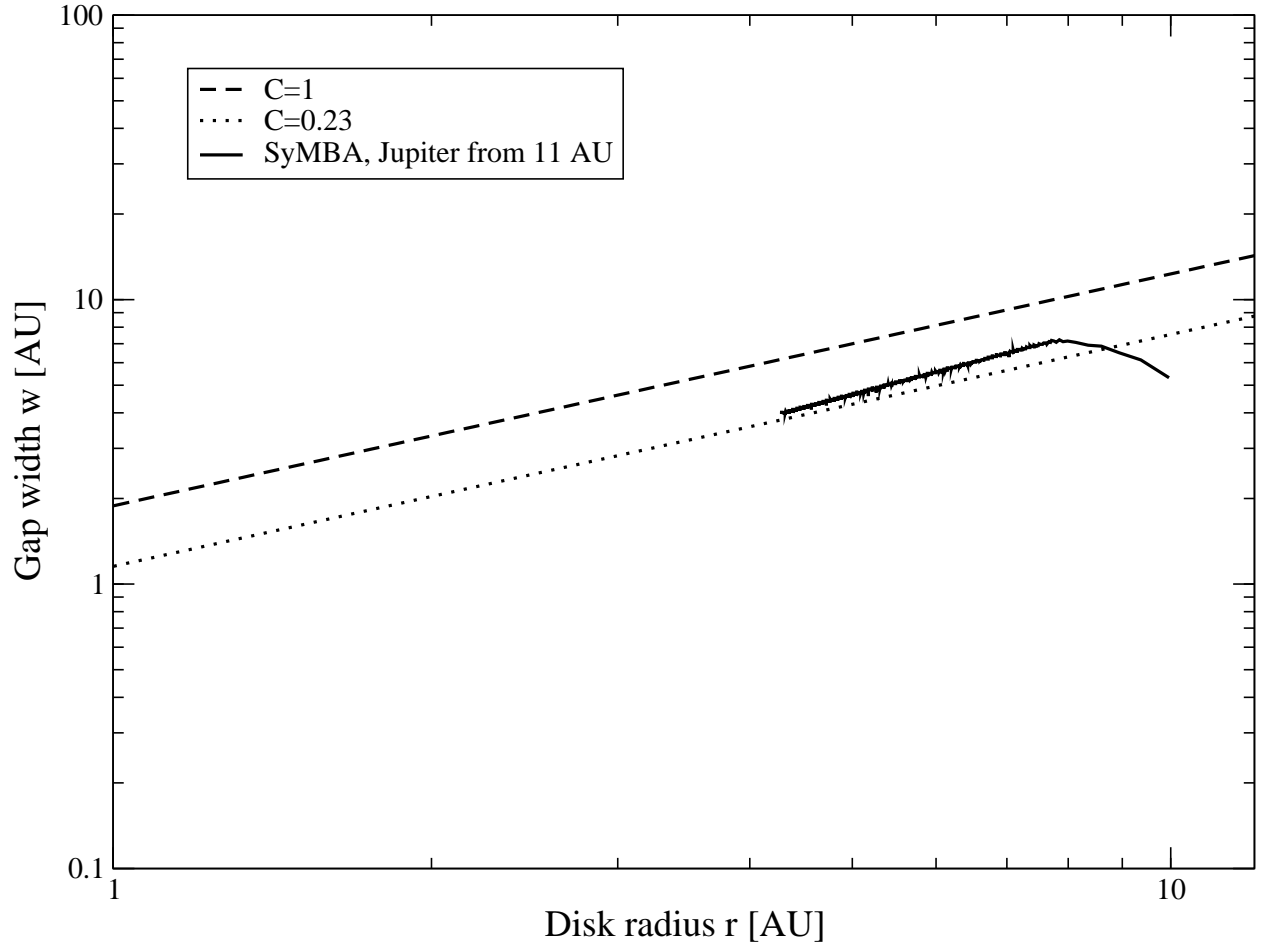


Fig. 9.— The gap width calculated by the Eq. 7 compared with the one determined from the simulations in Fig. 5. The dashed and dotted lines correspond to  $C = 1$  and  $C = 0.23$  respectively.

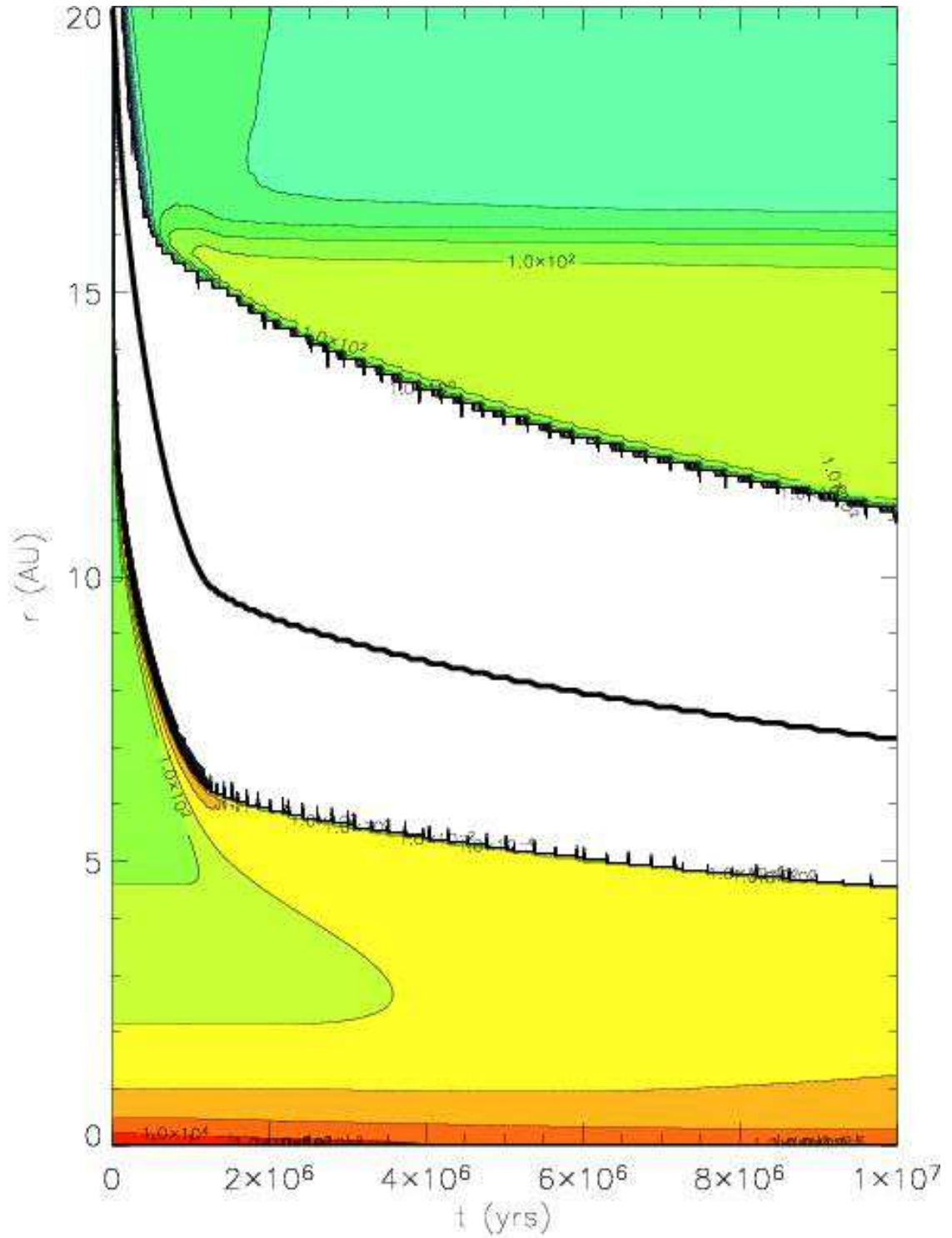


Fig. 10.— The same as Fig. 5, but the viscosity parameter is  $\alpha = 10^{-3}$  outside the dead zone and  $\alpha = 10^{-5}$  inside the dead zone. A Jupiter mass planet migrates into the dead zone, and slows down significantly after it opens a wide gap in the dead zone. The final orbital radius of the planet is  $\sim 7$  AU.

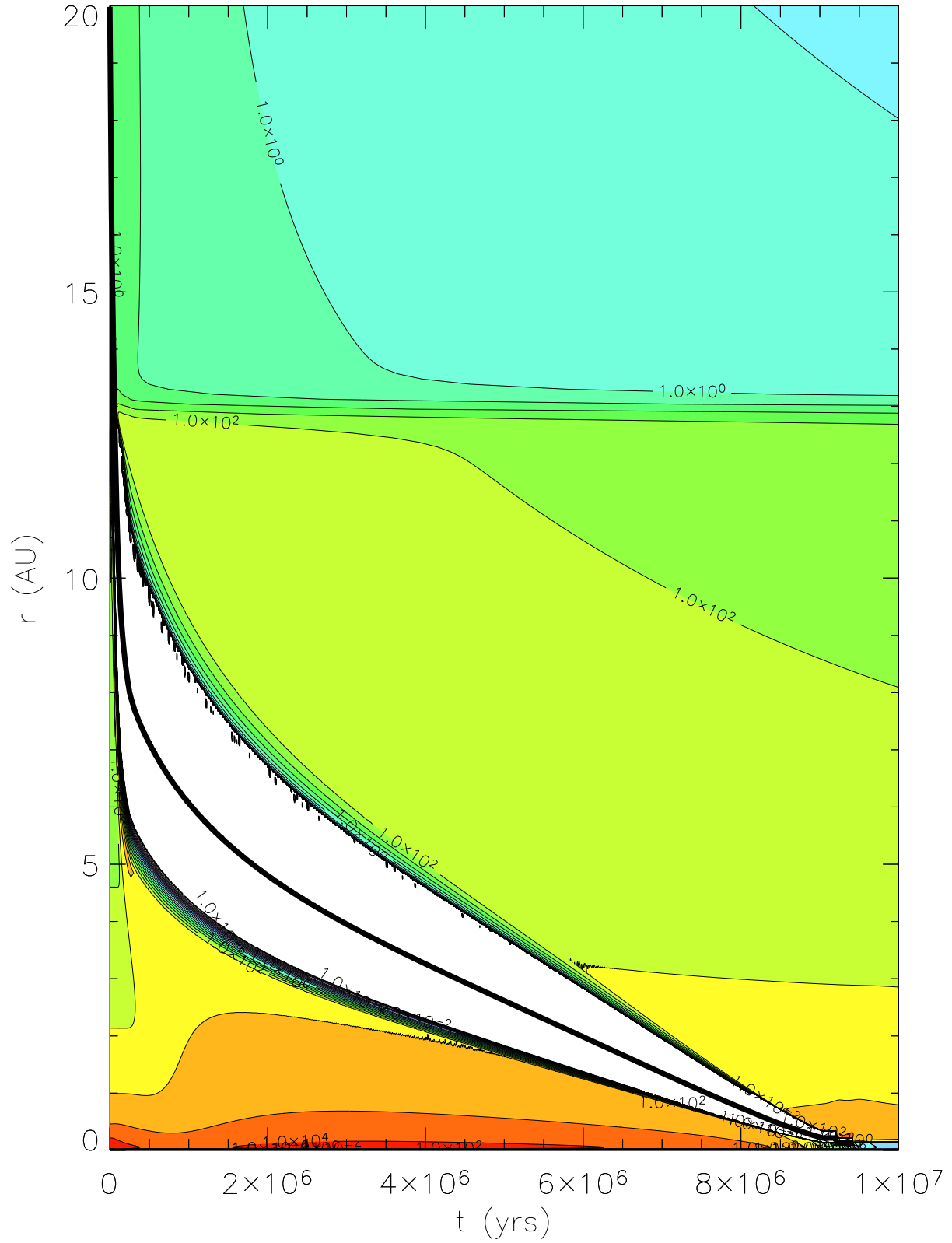


Fig. 11.— The same as Fig. 5, but the viscosity parameter is  $\alpha = 10^{-2}$  outside the dead zone and  $\alpha = 10^{-4}$  inside the dead zone. A Jupiter mass planet migrates into the dead zone

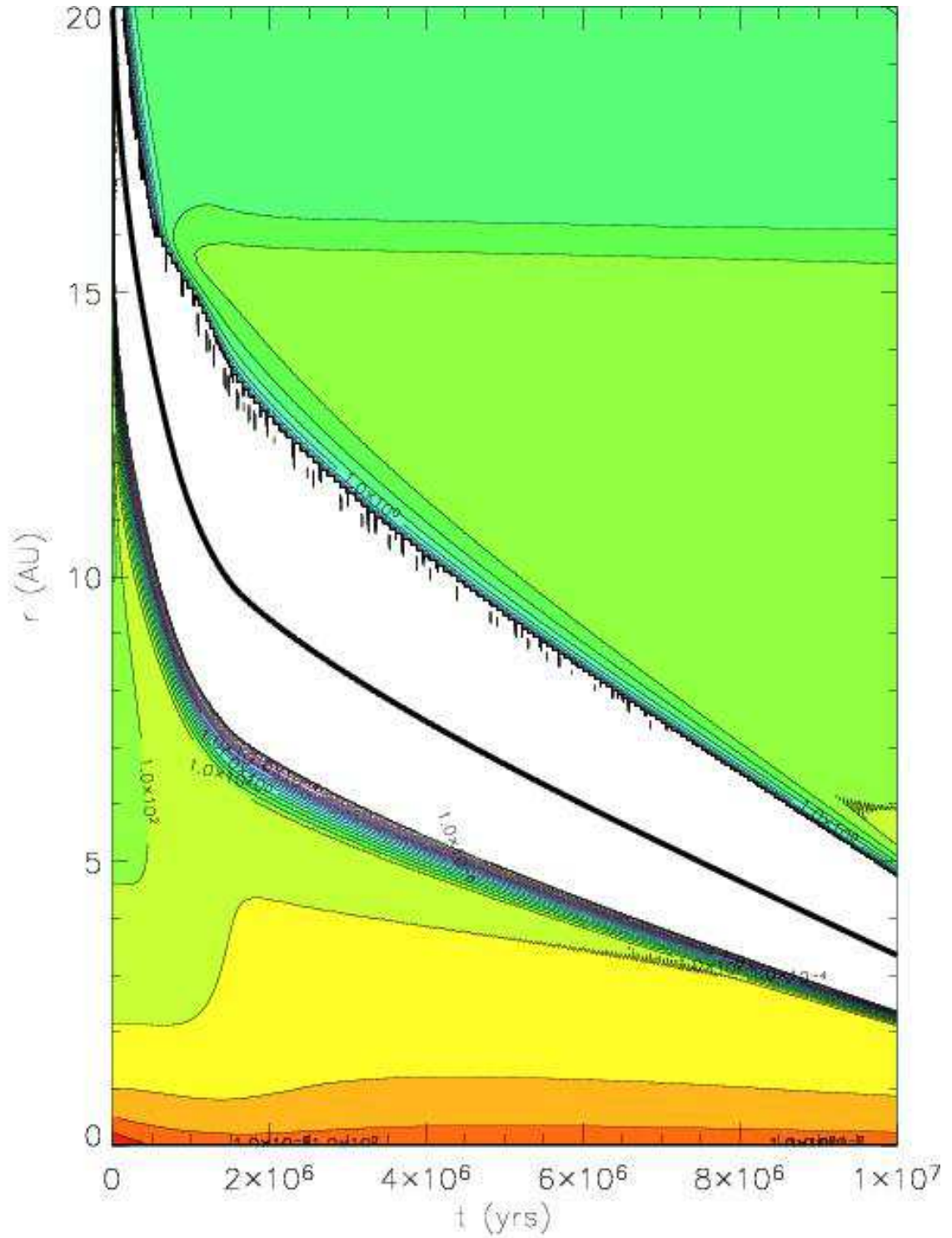


Fig. 12.— The same as Fig. 5, but the viscosity parameter is  $\alpha = 10^{-3}$  outside the dead zone and  $\alpha = 10^{-4}$  inside the dead zone. A Jupiter mass planet migrates into the dead zone as it opens a gap, but is not slowed as much as Fig. 5. The final orbital radius of the planet is  $\sim 3.5$  AU.

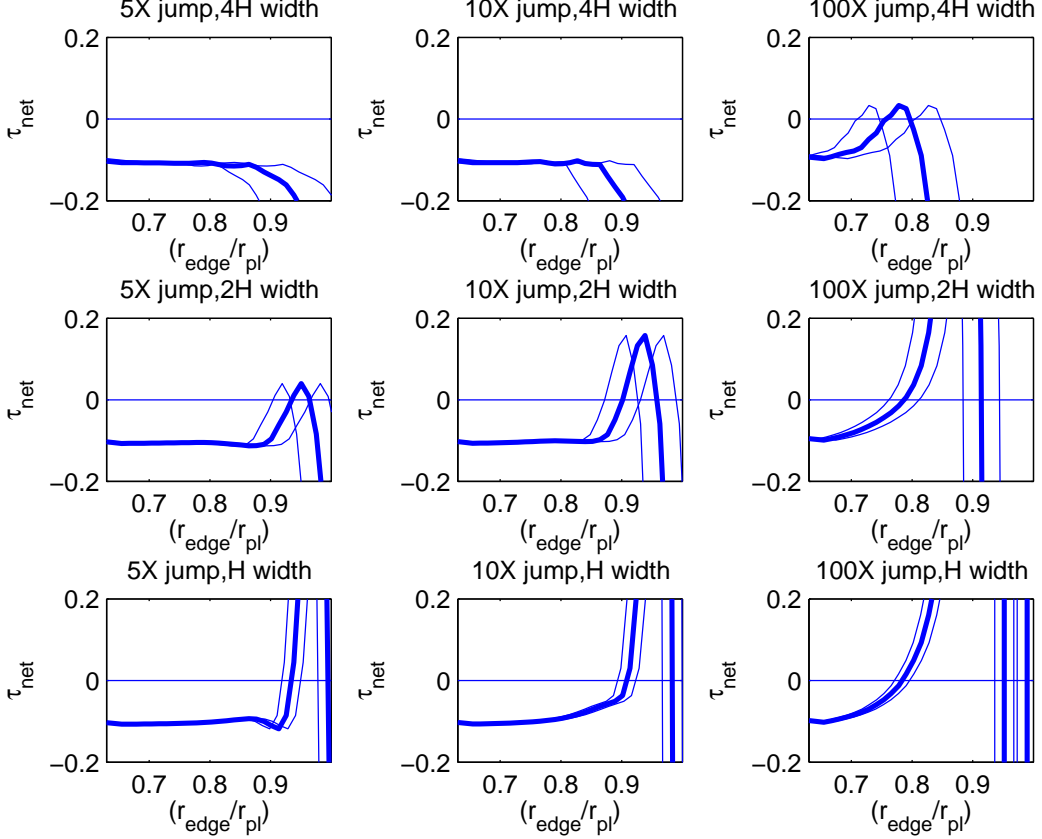


Fig. 13.— Normalized net torque  $\tau_{\text{net}}$  density on a planet embedded in a power-law gas disk containing a jump in surface. The planet has orbital radius  $r_{\text{pl}}$ , and the net torque felt by the planet is plotted as a function of the midpoint of the density jump,  $r_{\text{edge}}$ . Away from the edge, the gas disk surface density is a power law,  $\Sigma \propto r^{-3/2}$ . The calculation is carried out for density jump factors  $F = 5, 10, 100$ , occurring over a radial width  $\omega = h, 2h, 4h$  where  $h$  is the disk scale height at  $r_{\text{edge}}$  (see Eq. B1). The torques are computed two-dimensionally, i.e.  $B = 0$  in Eq. B8. The thick curve shows the net torque, while the horizontal distance between the thin curves on either side shows the corresponding radial width  $\omega$  of the density jump. Since  $\omega$  is scaled to  $h$  at  $r_{\text{edge}}$ , this changes as the edge midpoint changes.

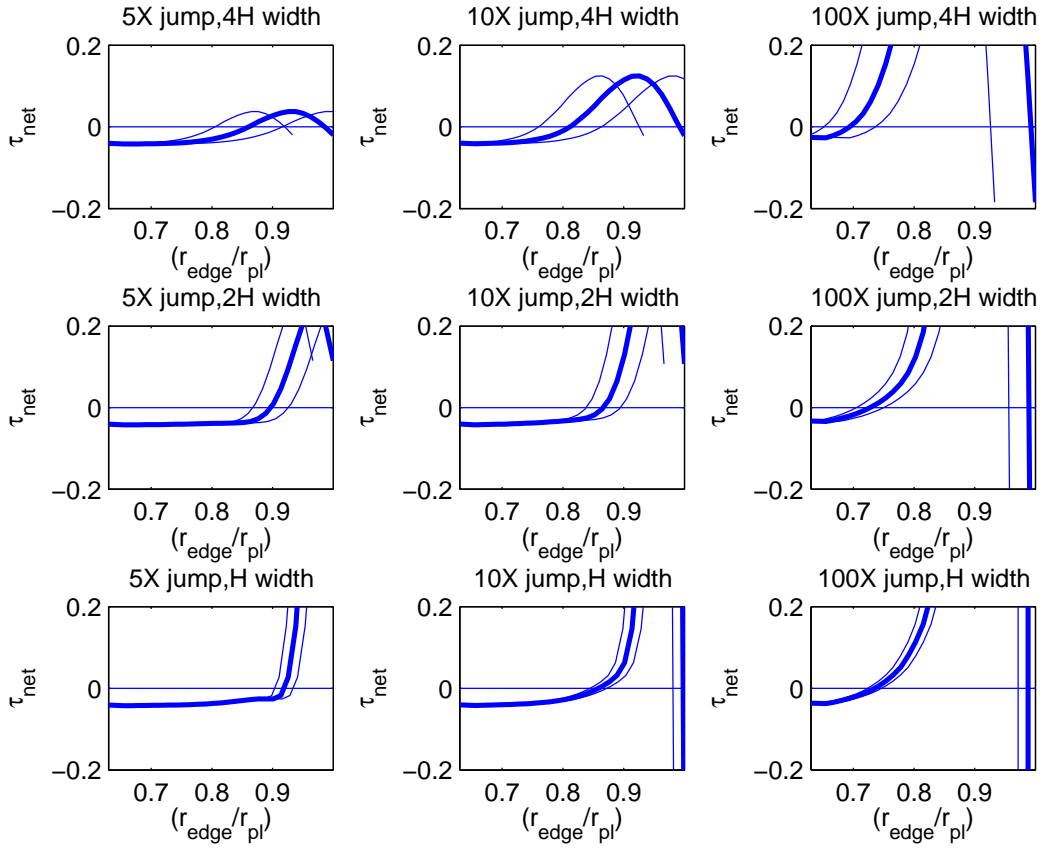


Fig. 14.— The computation shown in Fig. 13, repeated with  $B = 0.5$ , i.e. vertical softening of torques by half the disk scale height (Eq. B8).